

Flows *on* *$100 h^{-1}$ Mpc Scales*

Hume A. Feldman

Physics & Astronomy

University of Kansas

Peculiar Velocity Field

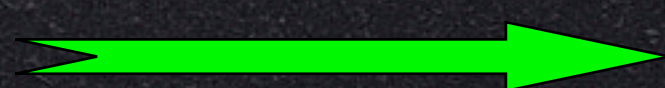
Measure the line of sight peculiar velocities:

$$v_p = cz - H_0 r$$

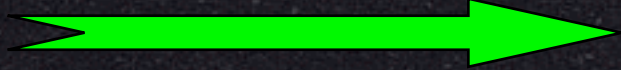
The difference between the redshift and the distance

Why should we study v_p ?

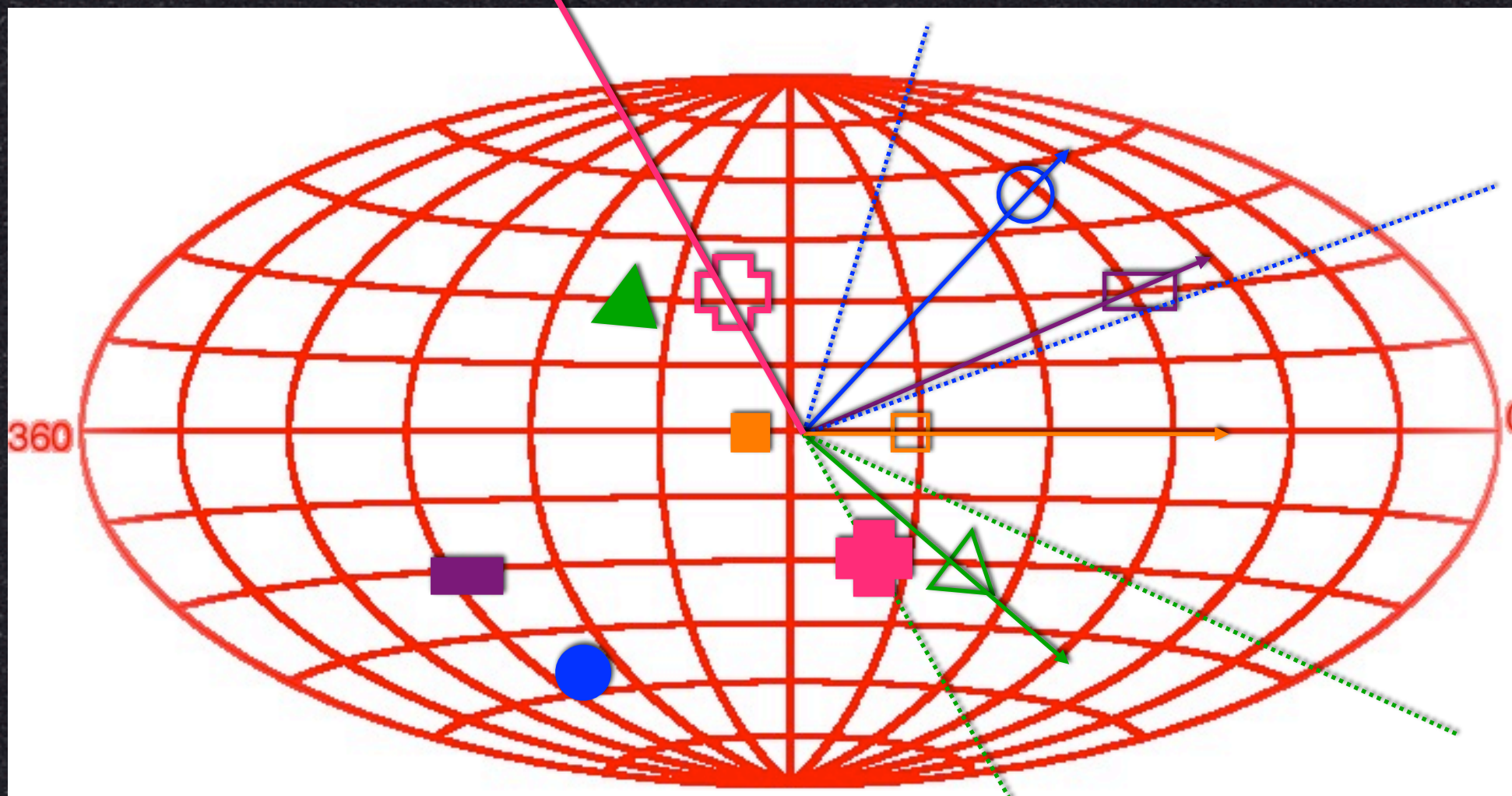
- ★ The peculiar velocity field is dominated by large scales



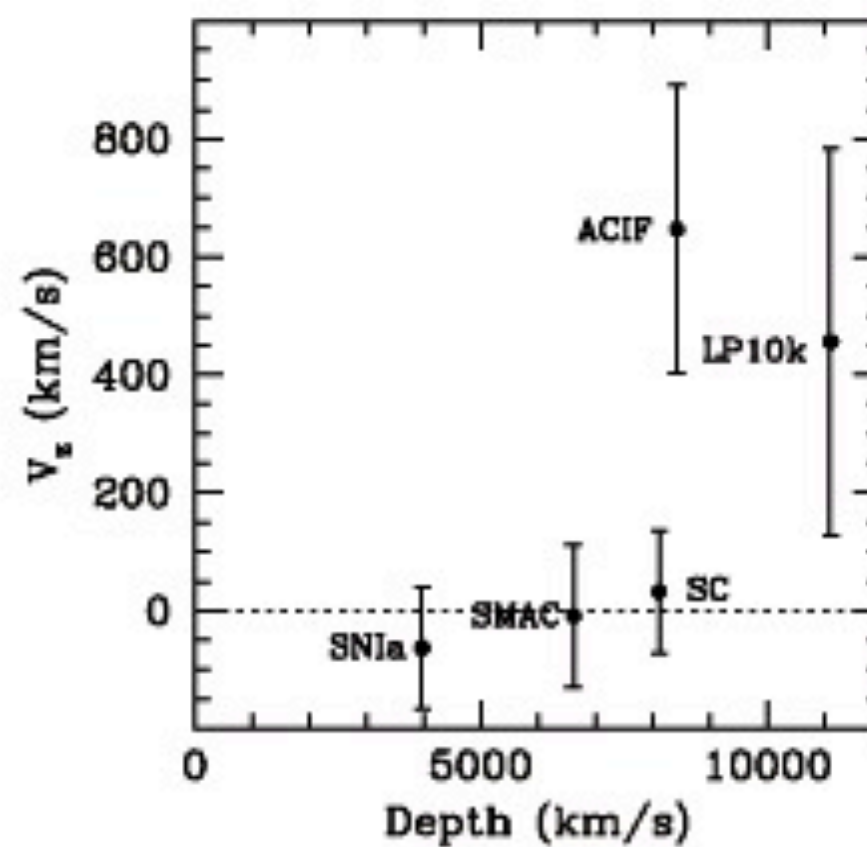
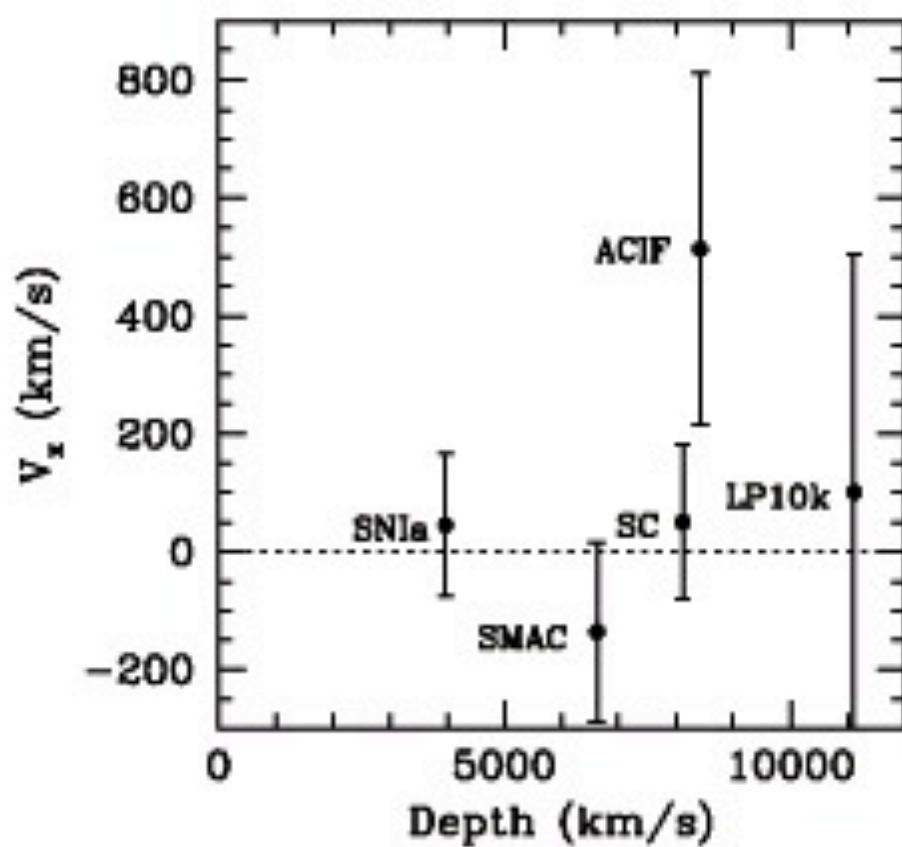
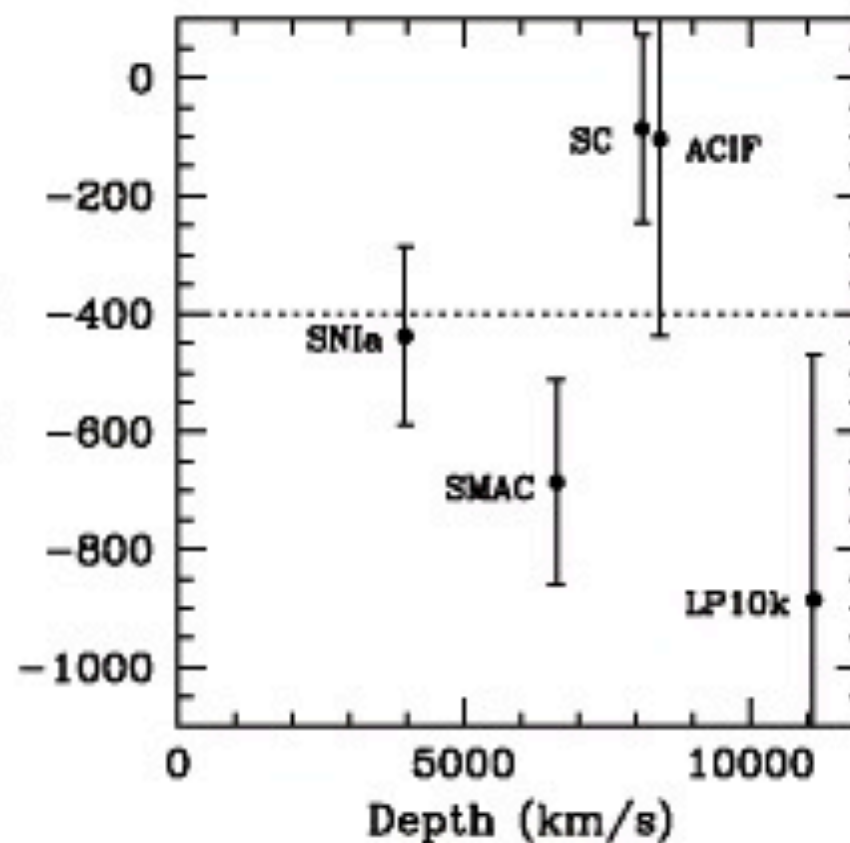
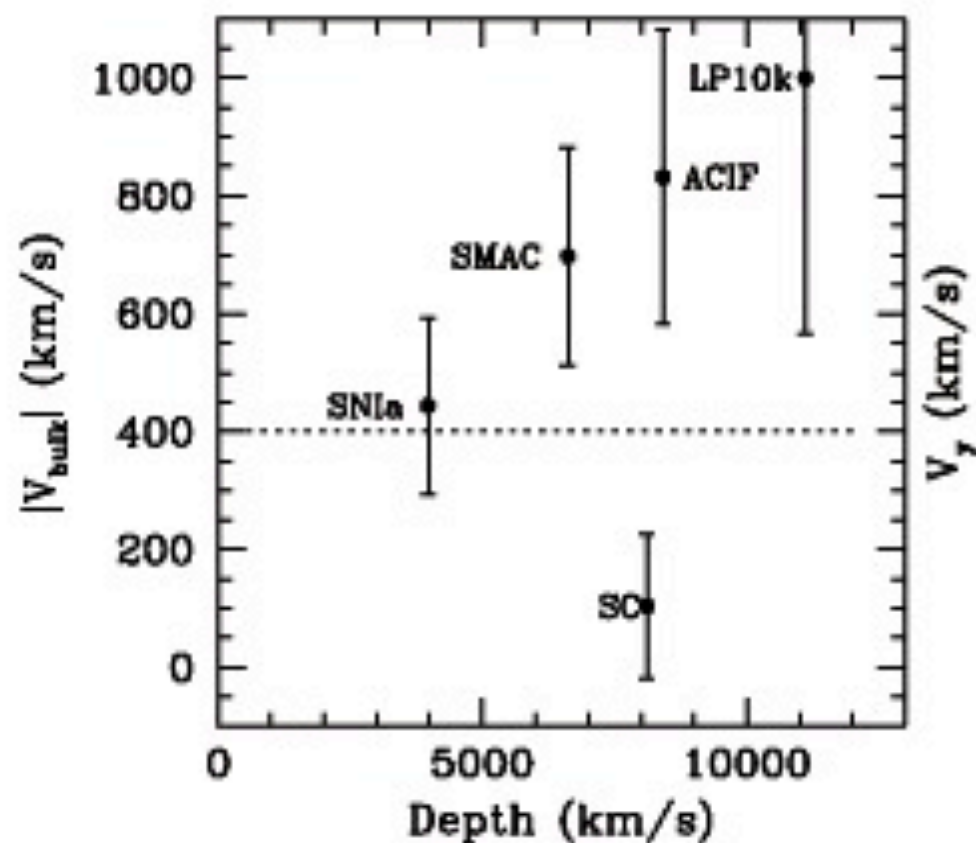
Linear structure

- ★ Test of gravitational instability model $\vec{\nabla} \cdot \vec{V} = \frac{\delta\rho}{\rho}$ $\vec{\nabla} \times \vec{V} = 0$
- ★ A direct probe of the mass distribution $\vec{V} = -\vec{\nabla}\phi$
- ★ Comparison of velocity fields & Luminous matter distribution  bias, Ω ...

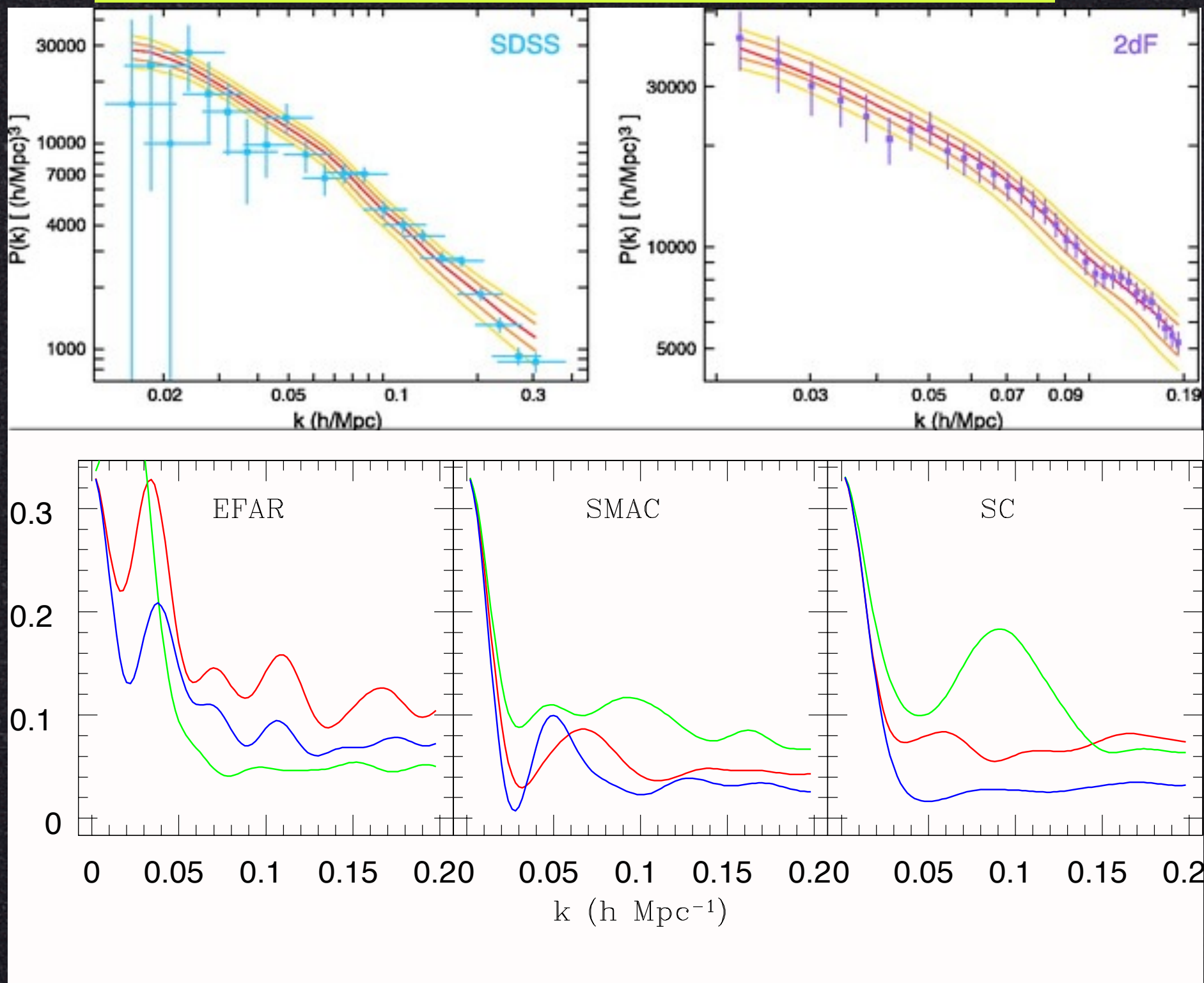
Local Group Velocity (Cautionary History Lesson)



Survey	l	b	$ V_{LG} $
V_{CMB}	271°	$+29^\circ$	620 km / s
V_{LP}	220°	-28°	$561 \pm 284 \text{ km / s}$
V_{RPK}	260°	$+54^\circ$	$600 \pm 350 \text{ km / s}$
V_{SMAC}	195°	0°	$700 \pm 250 \text{ km / s}$
V_{LP10k}	173°	$+63^\circ$	$1000 \pm 500 \text{ km / s}$
V_{SC}	180°	0°	$100 \pm 150 \text{ km / s}$



$$\tilde{p} = N \int \frac{d^3 k}{(2\pi)^3} p(\vec{k}) W(\vec{k})$$



Velocity Fields

The Modern Version

HAF, Watkins & Hudson, arXiv.0911.5516 (2009)

Watkins, HAF & Hudson, *MNRAS*, 392, 743-756 (2009)

HAF & Watkins, *MNRAS* 387, 825-829 (2008)

Watkins & HAF, *MNRAS* 379, 343-348 (2007)

Sarkar, HAF & Watkins, *MNRAS* 375 691-697 (2007)

Redshift-Distance surveys

- Construct the full three dimensional bulk-flow vectors.
- Compare bulk-flow for peculiar velocity surveys.
- Surveys differ in their
 - geometry
 - measurement errors
 - galaxy types.
- The overall errors are
 - Statistical
 - Systematic
 - Aliasing

The Physics of Velocity Fields

On scales that are small compared to the Hubble radius, galaxy motions are manifest in deviations from the idealized isotropic cosmological expansion

$$cz = H_0 r + \hat{\mathbf{r}} \cdot [\mathbf{v}(\mathbf{r}) - \mathbf{v}(0)]$$

The redshift-distance samples, obtained from peculiar velocity surveys, allow us to determine the radial (line-of-sight) component of the peculiar velocity of each galaxy:

$$v(r) = \hat{\mathbf{r}} \cdot \mathbf{v}(\mathbf{r}) = cz - H_0 r$$

The Physics of Velocity Fields

Galaxies trace the large-scale linear velocity field $\mathbf{v}(\mathbf{r})$ which is described by a Gaussian random field that is completely defined, in Fourier space, by its velocity power spectrum $P_v(k)$.

Fourier Transform of the line-of-sight velocity

$$\hat{\mathbf{r}} \cdot \mathbf{v}(\mathbf{r}) = \frac{1}{(2\pi)^3} \int d^3\mathbf{k} \hat{\mathbf{r}} \cdot \hat{\mathbf{k}} v(\mathbf{k}) e^{i\mathbf{k} \cdot \mathbf{r}}$$

Define the velocity power spectrum $P_v(k)$

$$\langle v(\mathbf{k}) v^*(\mathbf{k}') \rangle = (2\pi)^3 P_v(k) \delta_D(\mathbf{k} - \mathbf{k}')$$

The Physics of Velocity Fields

In linear theory, the velocity power spectrum is related to the density power spectrum

$$P_v(k) = \frac{H^2}{k^2} f^2(\Omega_{m,0}, \Omega_\Lambda) P(k)$$

The rate of growth of the perturbations at the present epoch

The Physics of Velocity Fields

In linear theory, the velocity power spectrum is related to the density power spectrum

$$P_v(k) = \frac{H^2}{k^2} f^2(\Omega_{m,0}, \Omega_\Lambda) P(k)$$

The power spectrum provides a complete statistical description of the linear peculiar velocity field.

Likelihood Methods for Peculiar Velocities

A catalog of peculiar velocities galaxies, labeled by an index n

Positions r_n

Estimates of the line-of-sight peculiar velocities S_n

Uncertainties σ_n

Assume that observational errors are Gaussian distributed.

Model the velocity field as a uniform streaming motion, or bulk flow, denoted by U , about which are random motions drawn from a Gaussian distribution with a 1-D velocity dispersion σ_*

Likelihood Methods for Peculiar Velocities

Likelihood function for the bulk flow components

$$L(U_i) = \prod_n \frac{1}{\sqrt{\sigma_n^2 + \sigma_*^2}} \exp \left(-\frac{1}{2} \frac{(S_n - \hat{r}_{n,i} U_i)^2}{\sigma_n^2 + \sigma_*^2} \right)$$

Maximum likelihood solution for bulk flow

$$U_i = A_{ij}^{-1} \sum_n \frac{\hat{r}_{n,j} S_n}{\sigma_n^2 + \sigma_*^2}$$

where

$$A_{ij} = \sum_n \frac{\hat{r}_{n,i} \hat{r}_{n,j}}{\sigma_n^2 + \sigma_*^2}$$

Likelihood Methods for Peculiar Velocities

The measured peculiar velocity of galaxy n

$$S_n = \hat{r}_{n,i} v_i(\mathbf{r}_n) + \epsilon_n$$

A Gaussian with zero mean
and variance $\sigma_n^2 + \sigma_*^2$

Theoretical
covariance matrix
for the bulk flow
components



$$R_{ij} = \langle v_i v_j \rangle = R_{ij}^{(v)} + \delta_{ij} (\sigma_i^2 + \sigma_*^2)$$

$$R_{ij}^{(v)} = \frac{1}{(2\pi)^3} \int P_{(v)}(k) W_{ij}^2(k) d^3 k$$

$$= \frac{H^2 f^2 (\Omega_0)}{2\pi^2} \int P(k) W_{ij}^2(k) dk$$

Likelihood Methods for Peculiar Velocities

Question: Are surveys consistent with each other?

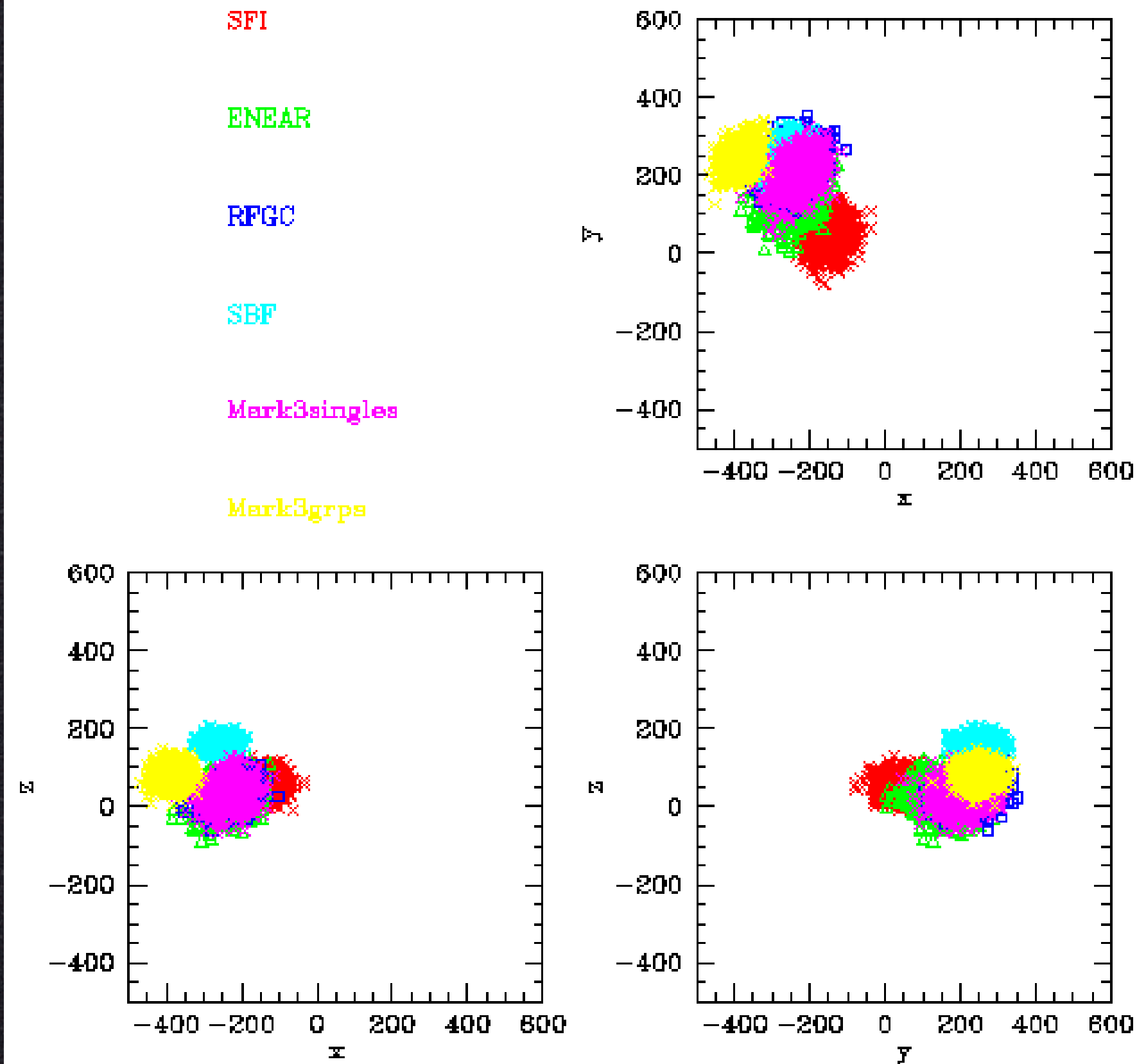
Even if two surveys are measuring the same underlying velocity field, they will not necessarily give the same bulk flow.

Reasons:

- ★ measurement errors in the peculiar velocities
- ★ surveys probe the velocity field in a different way

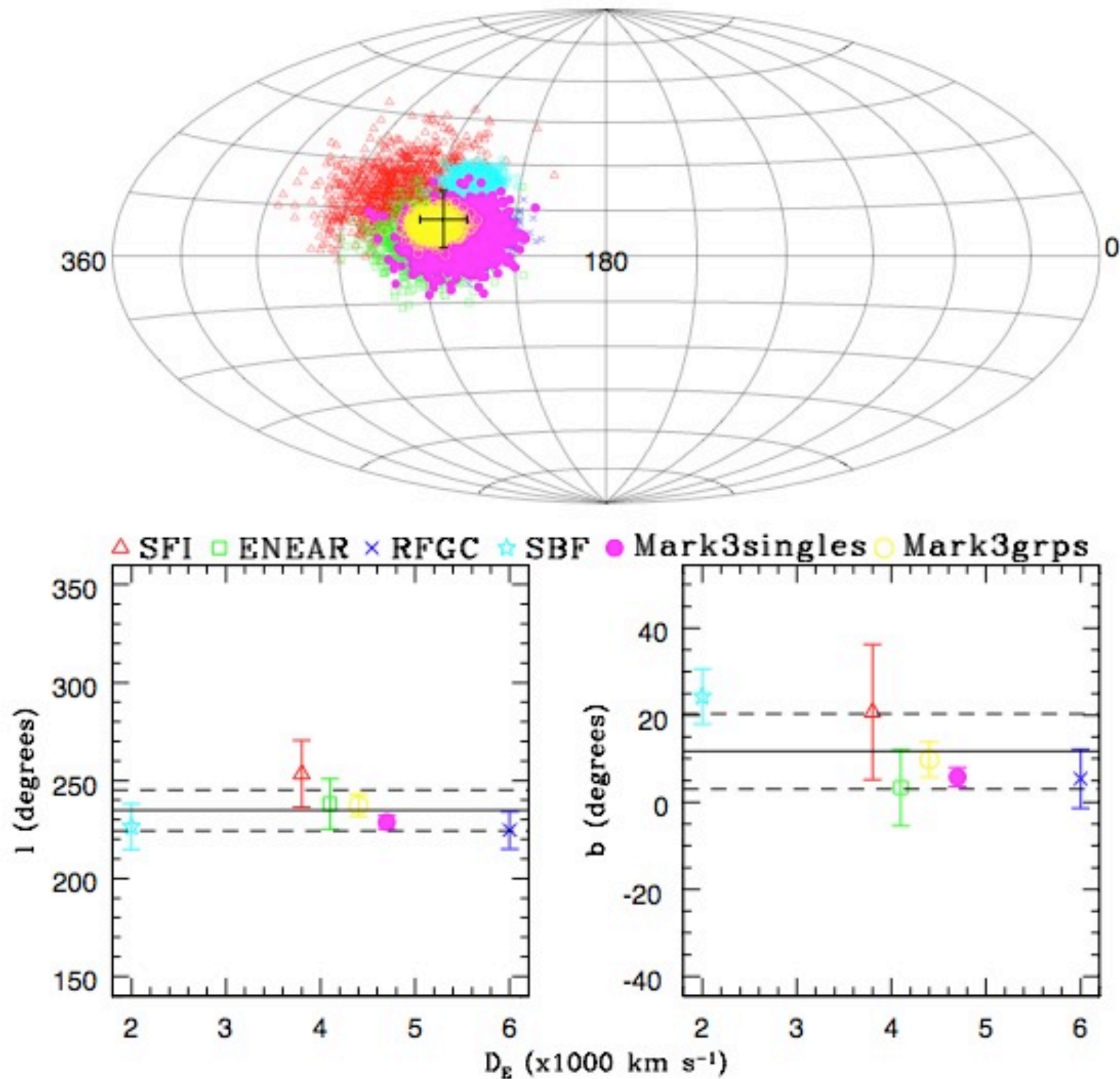
Comparing Velocity Field Surveys

Sarkar, HAF, Watkins, 2007



Comparing Velocity Field Surveys

Sarkar, HAF, Watkins, 2007

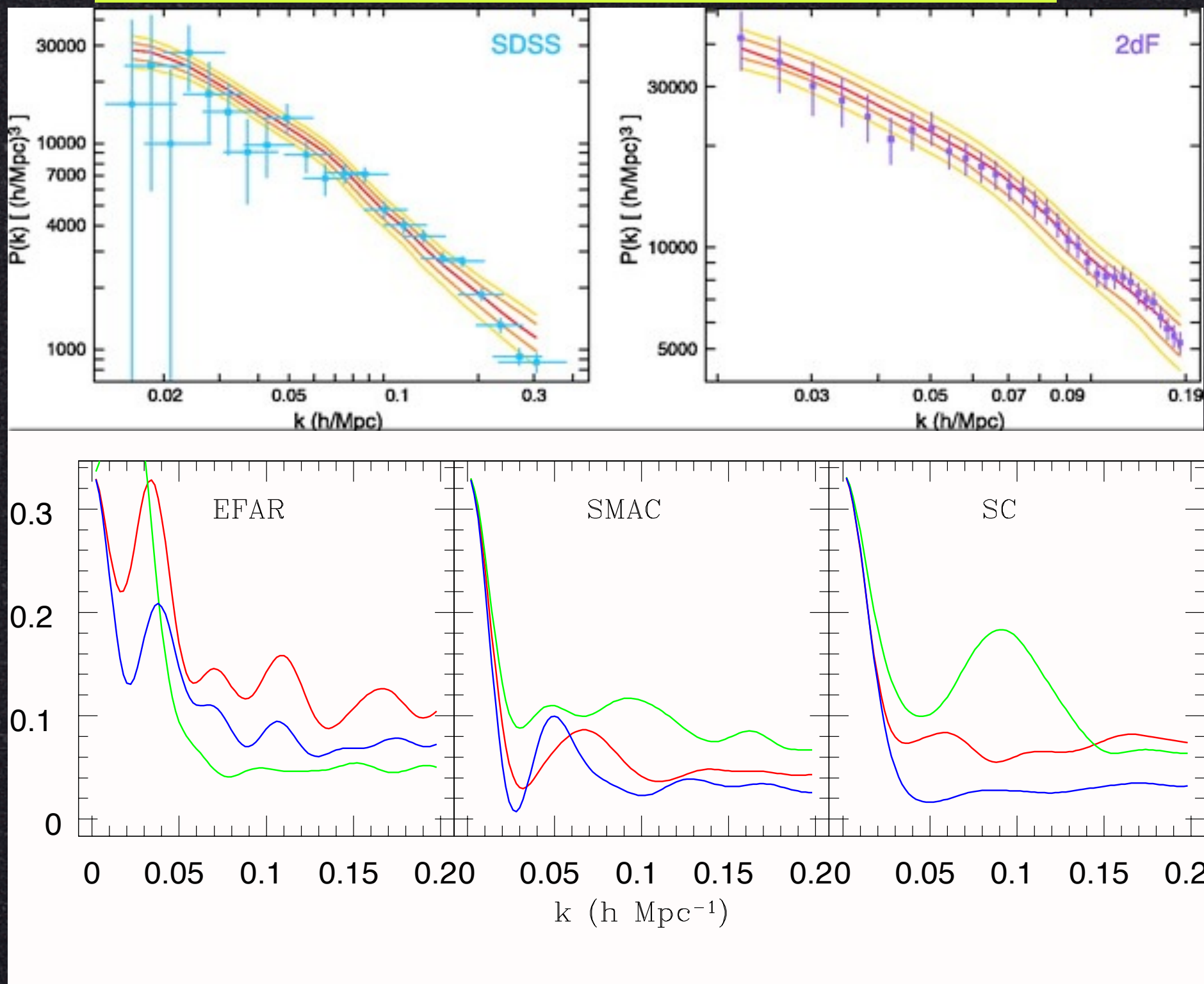


Can we do better?

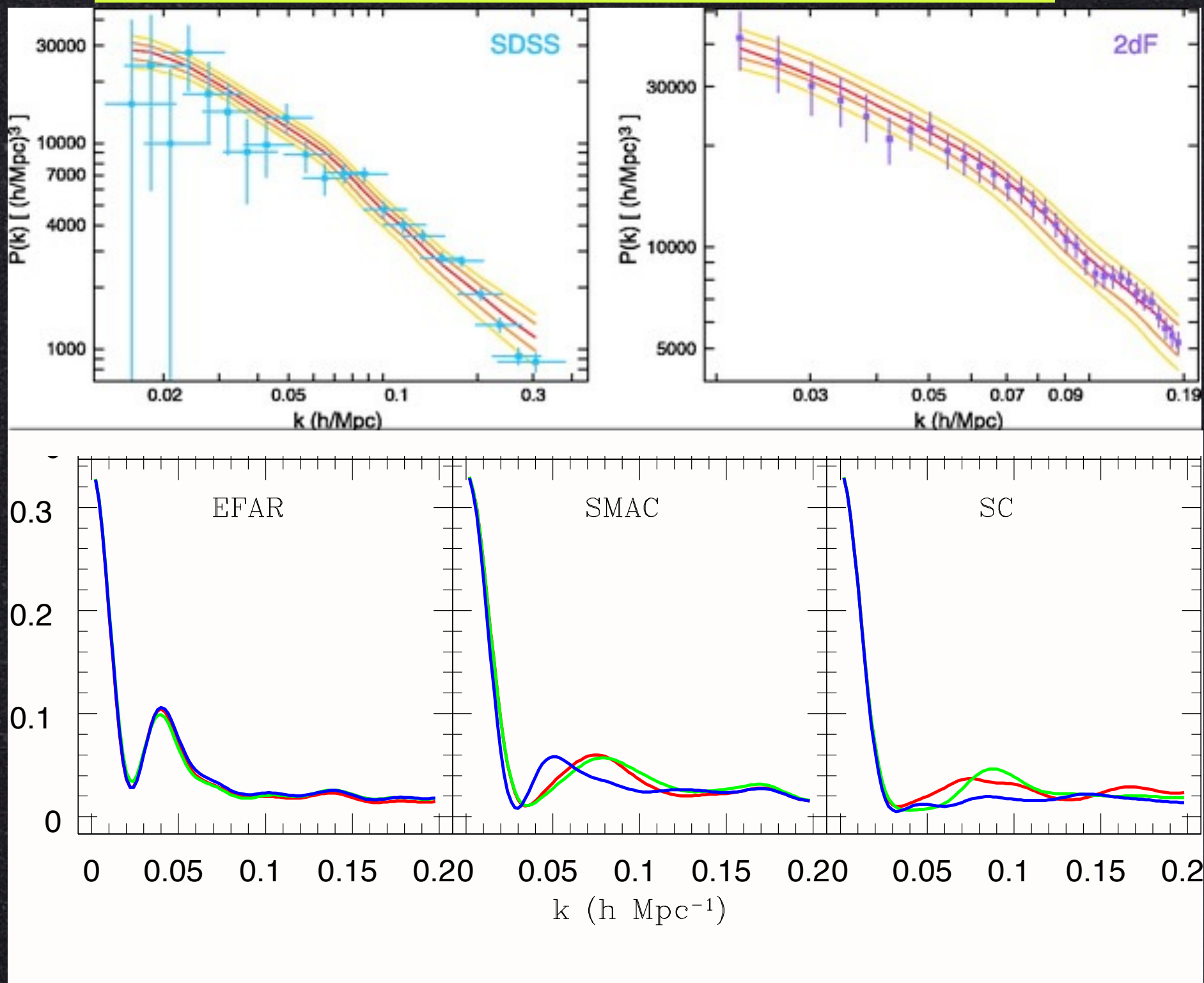
Get rid of small scale aliasing?

Improve the window
function design

$$\tilde{p} = N \int \frac{d^3 k}{(2\pi)^3} p(\vec{k}) W(\vec{k})$$



$$\tilde{p} = N \int \frac{d^3 k}{(2\pi)^3} p(\vec{k}) W(\vec{k})$$



Window Function Design

Decomposition of the velocity field

Kaiser 88, Jaffe & Kaiser 95

$$v_i(\mathbf{r}) = U_i + U_{ij}r_j + U_{ijk}r_jr_k + \dots$$

Bulk Flow

Shear

Octuple

If the velocity is a potential flow then both shear and octuple are symmetric (curl Free)

- > 3 DoF for BF
- > 6 DoF for shear
- > 10 DoF for Octuple



19 Independent components

Window Function Design

The BF Maximum Likelihood Estimates of the weights (MLE)

$$w_{i,n} = A_{ij}^{-1} \sum_n \frac{\mathbf{x}_j \cdot \mathbf{r}_n}{\sigma_n^2 + \sigma_*^2}$$

depends on the spatial distribution and the errors.

Goal:

- Study motions on largest scales
- Require WF that
 - have narrow peaks
 - small amplitude outside peak

Window Function Design

Consider an ideal survey

- Very large number of points
- Isotropic distribution
- Gaussian falloff $n(r) \propto \exp(-r^2/2R_I^2)$

R_I Depth of the survey

Find the weights that specify the moments

$$u_i = \sum_n w_{i,n} S_n$$

that minimize the variance $\langle (u_i - U_i)^2 \rangle$

Window Function Design

BF and shear moments are orthogonal by design
Higher moments are not.

e.g.: A pure octupole flow in a given volume V

$$v_i = U_{ijk} r_i r_k$$

contains a net bulk flow

$$\int_V U_{ijk} r_i r_k d^3 r$$

Which leads to a strong correlation between
the bulk flow and octupole moments

Window Function Design

Redefine the octuple moments

$$v_i(\mathbf{r}) = U_i + U_{ij}r_j + U_{ijk}(r_jr_k - \Lambda_{jk}) + \dots$$

where

$$\Lambda_{jk} = \int_V r_j r_k d^3r$$

For a spherically symmetric volume
only Λ_{ii} are non-zero

Window Function Design

Line-of-sight peculiar velocity

$$\begin{aligned}
 s(\mathbf{r}) &= \vec{v} \cdot \hat{r} \\
 &= U_i \hat{r}_i + U_{ij} r \hat{r}_i \hat{r}_j + U_{ijk} (r^2 \hat{r}_i \hat{r}_j \hat{r}_k - \Lambda_{jk} \hat{r}_i) + \dots \\
 &= \sum_{p=1}^{19} U_p g_p(\mathbf{r})
 \end{aligned}$$

Where

$$\begin{aligned}
 U_p = \{ & U_1, U_2, U_3, U_{11}, U_{22}, U_{33}, U_{12}, U_{23}, U_{13}, U_{111}, \\
 & U_{222}, U_{333}, U_{112}, U_{223}, U_{331}, U_{122}, U_{233}, U_{113}, U_{123} \}
 \end{aligned}$$

and

$$\begin{aligned}
 g_p(\mathbf{r}) = \{ & \hat{r}_1, \hat{r}_2, \hat{r}_3, r \hat{r}_1^2, r \hat{r}_2^2, r \hat{r}_3^2, 2r \hat{r}_1 \hat{r}_2, 2r \hat{r}_2 \hat{r}_3, 2r \hat{r}_1 \hat{r}_3, \\
 & r^2 \hat{r}_1^3 - \Lambda_{11} \hat{r}_1, r^2 \hat{r}_2^3 - \Lambda_{22} \hat{r}_2, r^2 \hat{r}_3^3 - \Lambda_{33} \hat{r}_3, 3r^2 \hat{r}_1^2 \hat{r}_2 - \Lambda_{11} \hat{r}_2, 3r^2 \hat{r}_2^2 \hat{r}_3 - \Lambda_{22} \hat{r}_3, \\
 & 3r^2 \hat{r}_3^2 \hat{r}_1 - \Lambda_{33} \hat{r}_1, 3r^2 \hat{r}_2^2 \hat{r}_1 - \Lambda_{22} \hat{r}_1, 3r^2 \hat{r}_3^2 \hat{r}_2 - \Lambda_{33} \hat{r}_2, 3r^2 \hat{r}_1^2 \hat{r}_3 - \Lambda_{11} \hat{r}_3, 6r^2 \hat{r}_1 \hat{r}_2 \hat{r}_3 \}
 \end{aligned}$$

Window Function Design

Ideal velocity moments

$$U_p = \frac{1}{N_o} \sum_{n=1}^{N_o} g_p(\mathbf{r}_n) s_n = \sum_n w'_{p,n} s_n \quad \text{where} \quad w'_{p,n} = \frac{g_p(\mathbf{r}_n)}{N_o}$$

Given U_p , find the weights $w_{p,n}$ such that

$$u_p = \sum_{n=1}^N w_{p,n} s_n \quad \text{gives the best possible estimates of } U_p$$

\Rightarrow On average, the correct amplitudes $\langle u_p \rangle = U_p$
for the velocity moments

Require that $\sum_n w_{p,n} g_q(\mathbf{r}_n) = \delta_{pq}$

Window Function Design

Enforce this constraint using Lagrange multiplier

$$\langle (U_p - u_p)^2 \rangle + \sum_q \lambda_{pq} \left(\sum_n w_{p,n} g_q(\mathbf{r}_n) - \delta_{pq} \right)$$

or expand out the variance

$$\langle U_p^2 \rangle - \sum_n 2w_{p,n} \langle S_n U_p \rangle + \sum_{n,m} w_{p,n} w_{p,m} \langle S_n S_m \rangle + \sum_q \lambda_{pq} \left(\sum_n w_{p,n} g_q(\mathbf{r}_n) - \delta_{pq} \right)$$

Minimize with respect to $w_{p,n}$

Window Function Design

$$-2\langle S_n U_p \rangle + 2 \sum_m w_{p,m} \langle S_n S_m \rangle + \sum_q \lambda_{pq} g_q(\mathbf{r}_n) = 0$$

$$w_{p,n} = \sum_m G_{nm}^{-1} \left(\langle S_m U_p \rangle - \frac{1}{2} \sum_q \lambda_{pq} g_q(\mathbf{r}_m) \right)$$

$$\mathbf{G}_{nm} = \langle S_n S_m \rangle \quad \text{individual velocity covariance matrix}$$

$$\lambda_{pq} = M_{pl}^{-1} \left(\sum_{m,n} G_{nm}^{-1} \langle S_m U_l \rangle g_q(\mathbf{r}_n) - \delta_{lq} \right)$$

$$M_{pq} = \frac{1}{2} \sum_{n,m} G_{nm}^{-1} g_p(\mathbf{r}_n) g_q(\mathbf{r}_m)$$

Window Function Design

The covariance matrix

$$\begin{aligned} G_{nm} &= \langle s_n s_m \rangle + \delta_{nm} (\sigma_*^2 + \sigma_n^2) \\ &= \langle \hat{\mathbf{r}}_n \cdot \mathbf{v}(\mathbf{r}_n) \quad \hat{\mathbf{r}}_m \cdot \mathbf{v}(\mathbf{r}_m) \rangle + \delta_{nm} (\sigma_*^2 + \sigma_n^2). \end{aligned}$$

The cross correlation

$$\langle S_m U_p \rangle = \sum_{n'} w'_{pn'} \langle s_m s_{n'} \rangle$$

Window Function Design

The correlation matrix

$$\begin{aligned} R_{pq} = \langle u_p u_q \rangle &= \sum_{nm} w_{pn} w_{qm} \langle s_n s_m \rangle = \sum_{nm} w_{pn} w_{qm} G_{nm} \\ &= R_{pq}^{(v)} + R_{pq}^{(\epsilon)} \end{aligned}$$

Velocity correlation matrix

$$R_{pq}^{(v)} = \frac{\Omega_m^{1.1}}{2\pi^2} \int dk P(k) \mathcal{W}_{pq}^2(k)$$

Noise correlation matrix

$$R_{pq}^{(\epsilon)} = \sum_n w_{pn} w_{qn} (\sigma_n^2 + \sigma_*^2)$$

Window Function Design

Tensor square window function

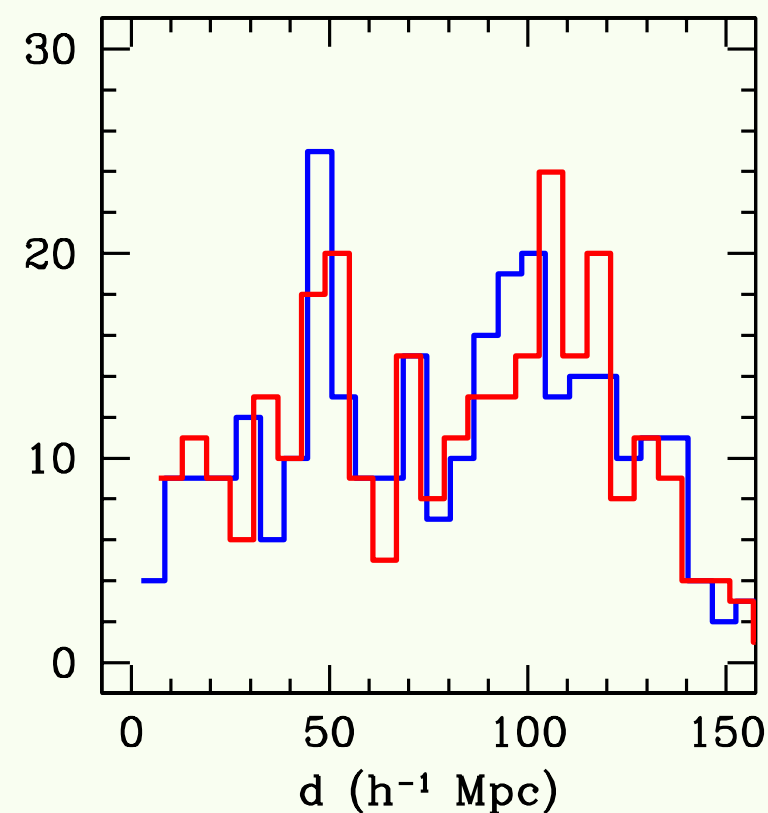
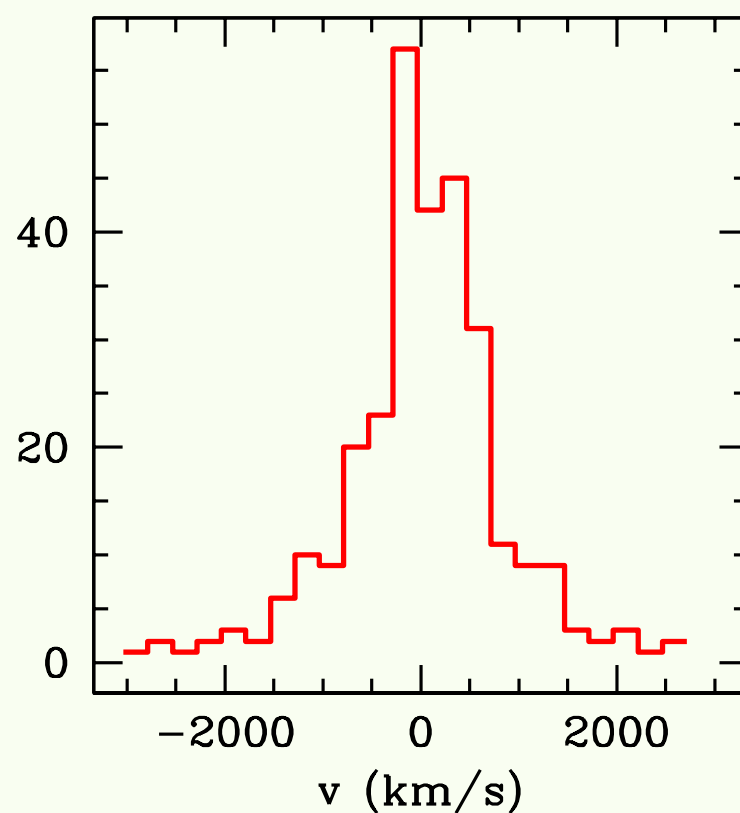
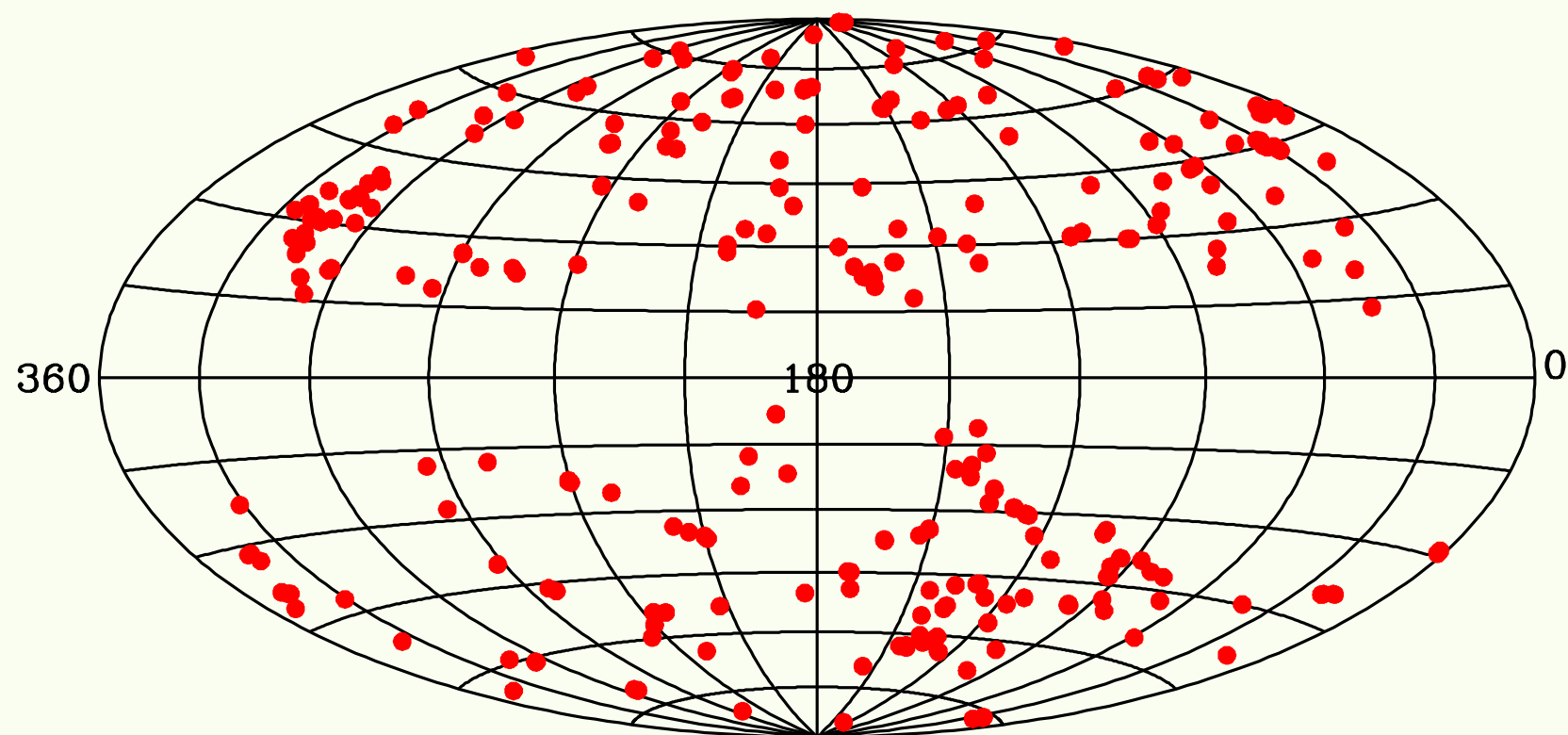
$$\mathcal{W}_{pq}^2 = \sum_{n,m} w_{pn} w_{qm} f_{nm}(k)$$

where

$$f_{mn}(k) = \int \frac{d^2 \hat{k}}{4\pi} \left(\hat{\mathbf{r}}_n \cdot \hat{\mathbf{k}} \right) \left(\hat{\mathbf{r}}_m \cdot \hat{\mathbf{k}} \right) \exp \left(ik \hat{\mathbf{k}} \cdot (\mathbf{r}_n - \mathbf{r}_m) \right)$$

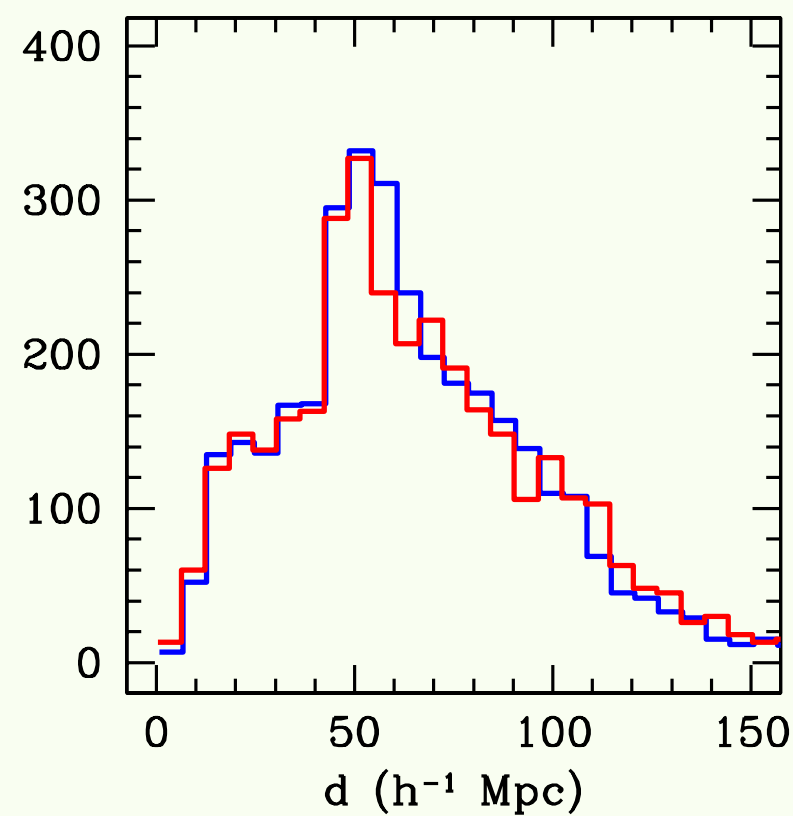
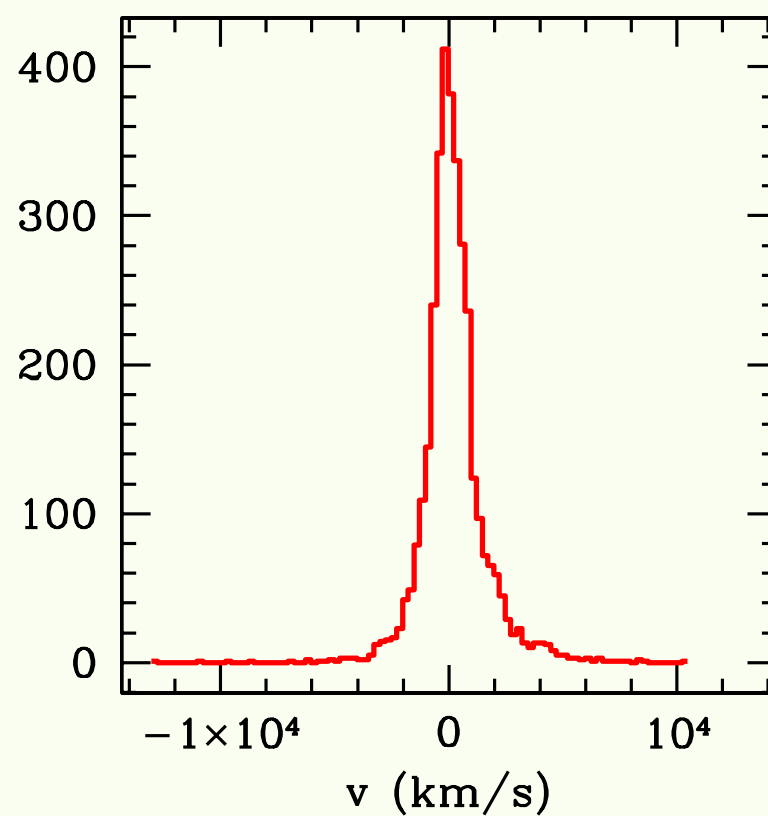
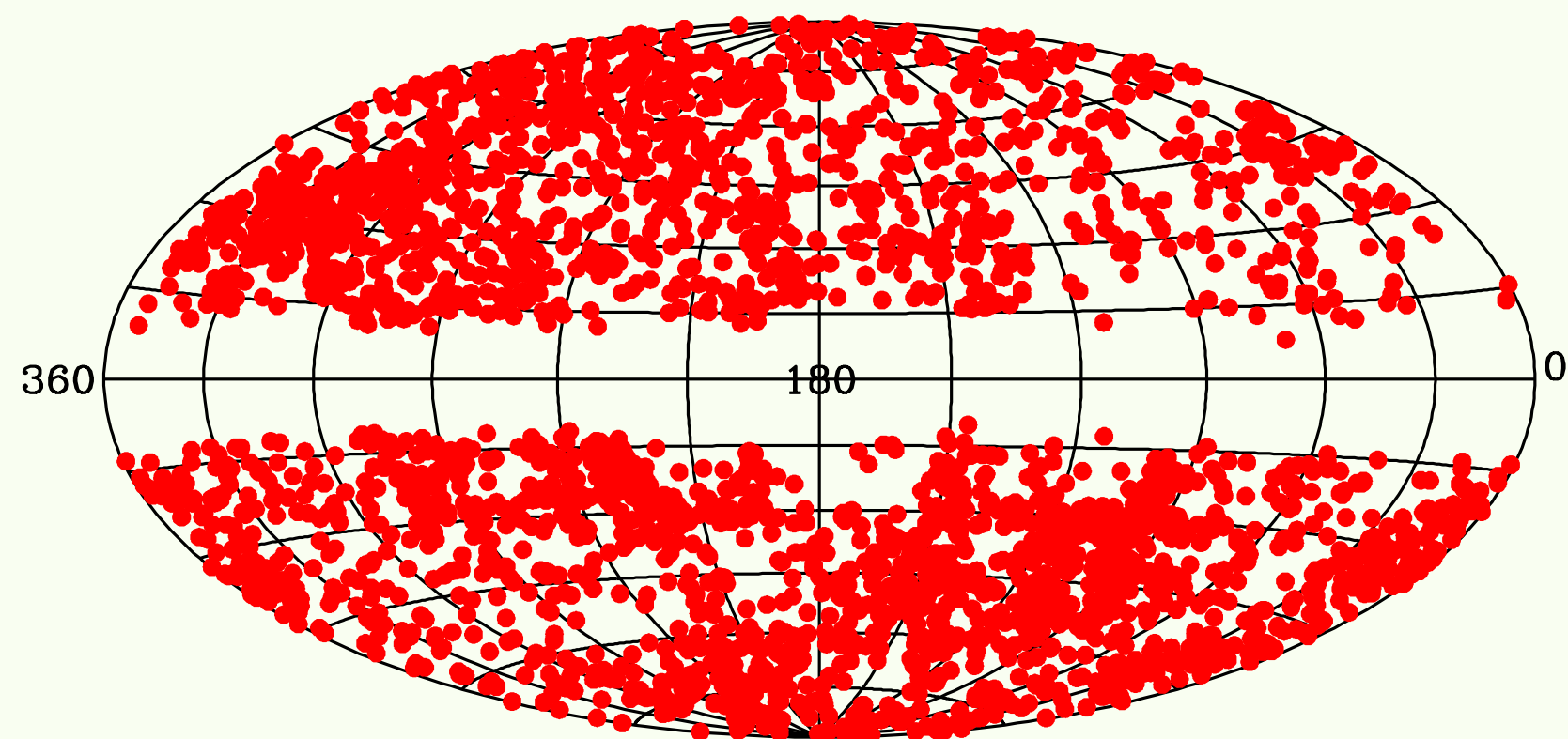
Peculiar Velocity Surveys

DEEP (294 Galaxies & Clusters)



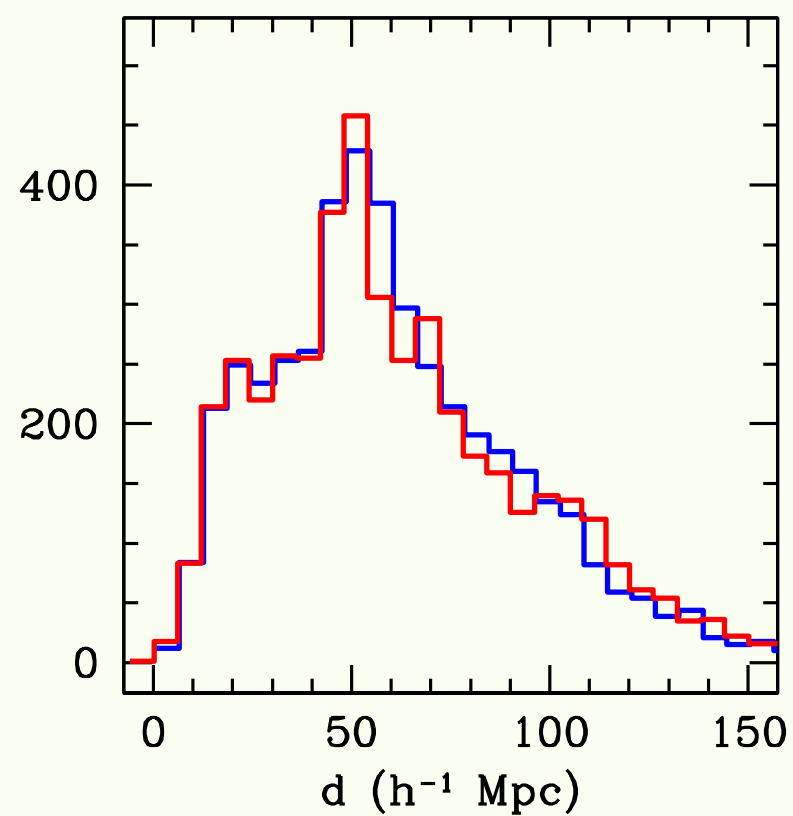
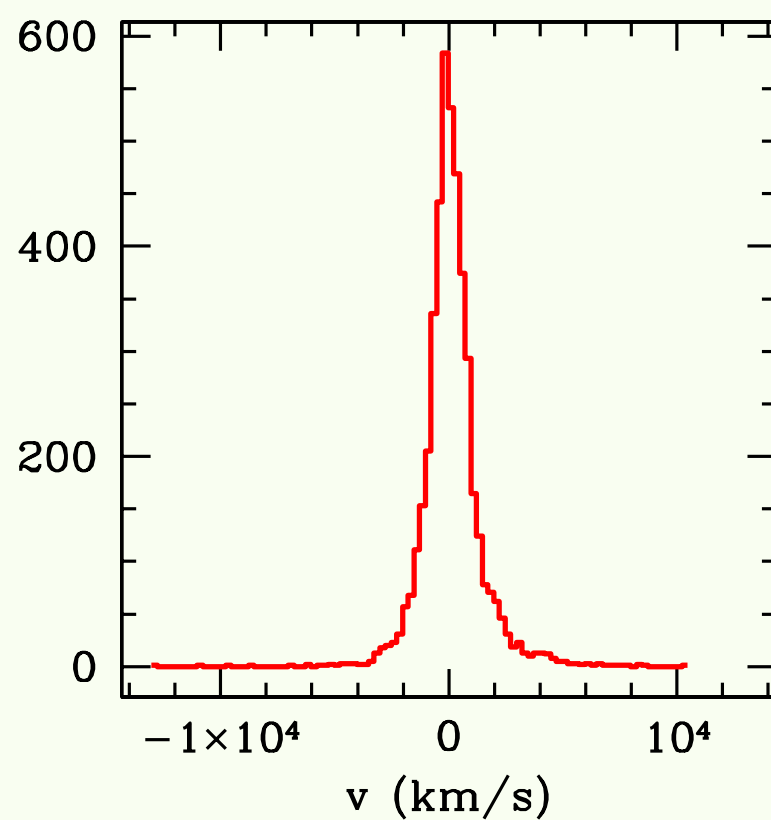
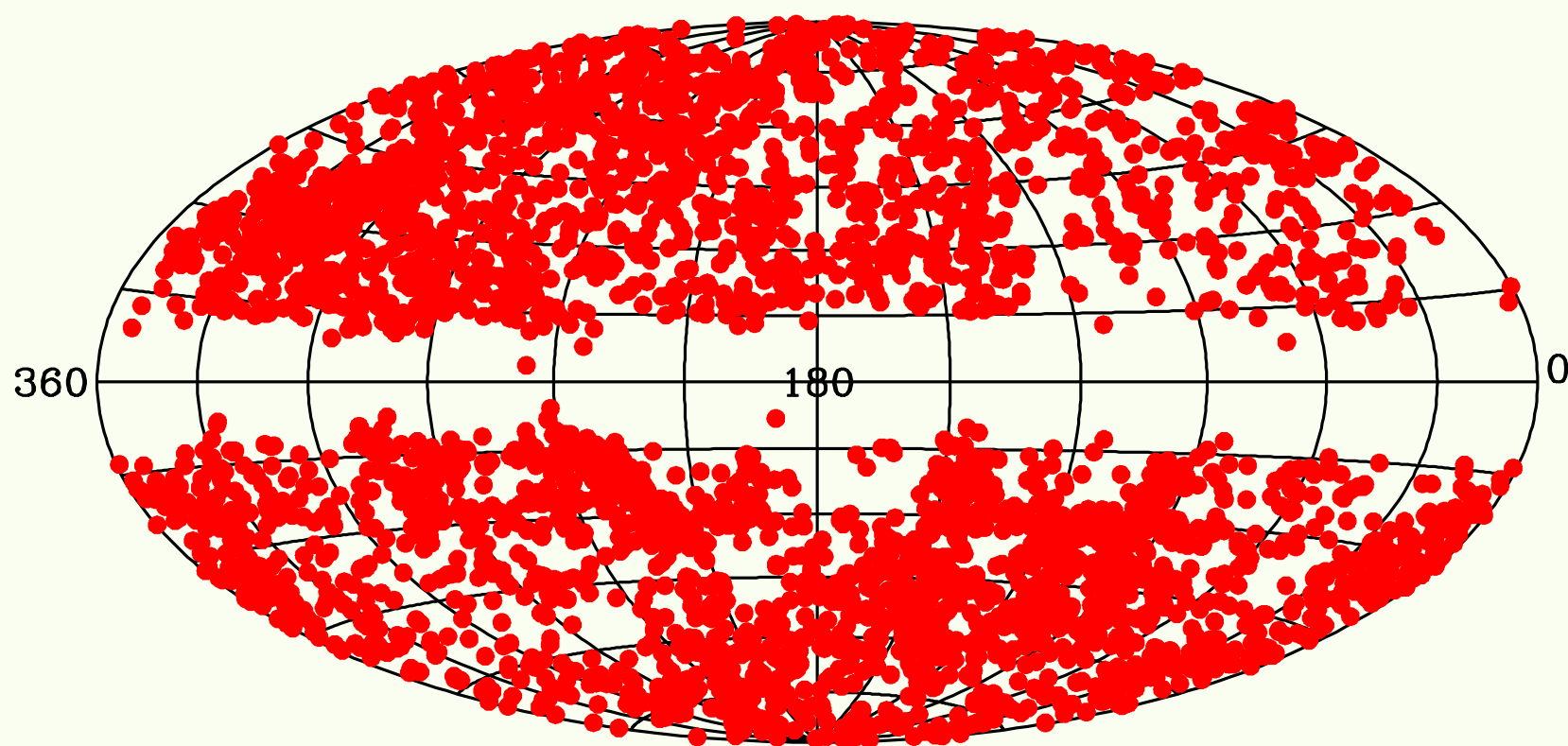
Peculiar Velocity Surveys

SFI++ (3401 Galaxies & Groups)

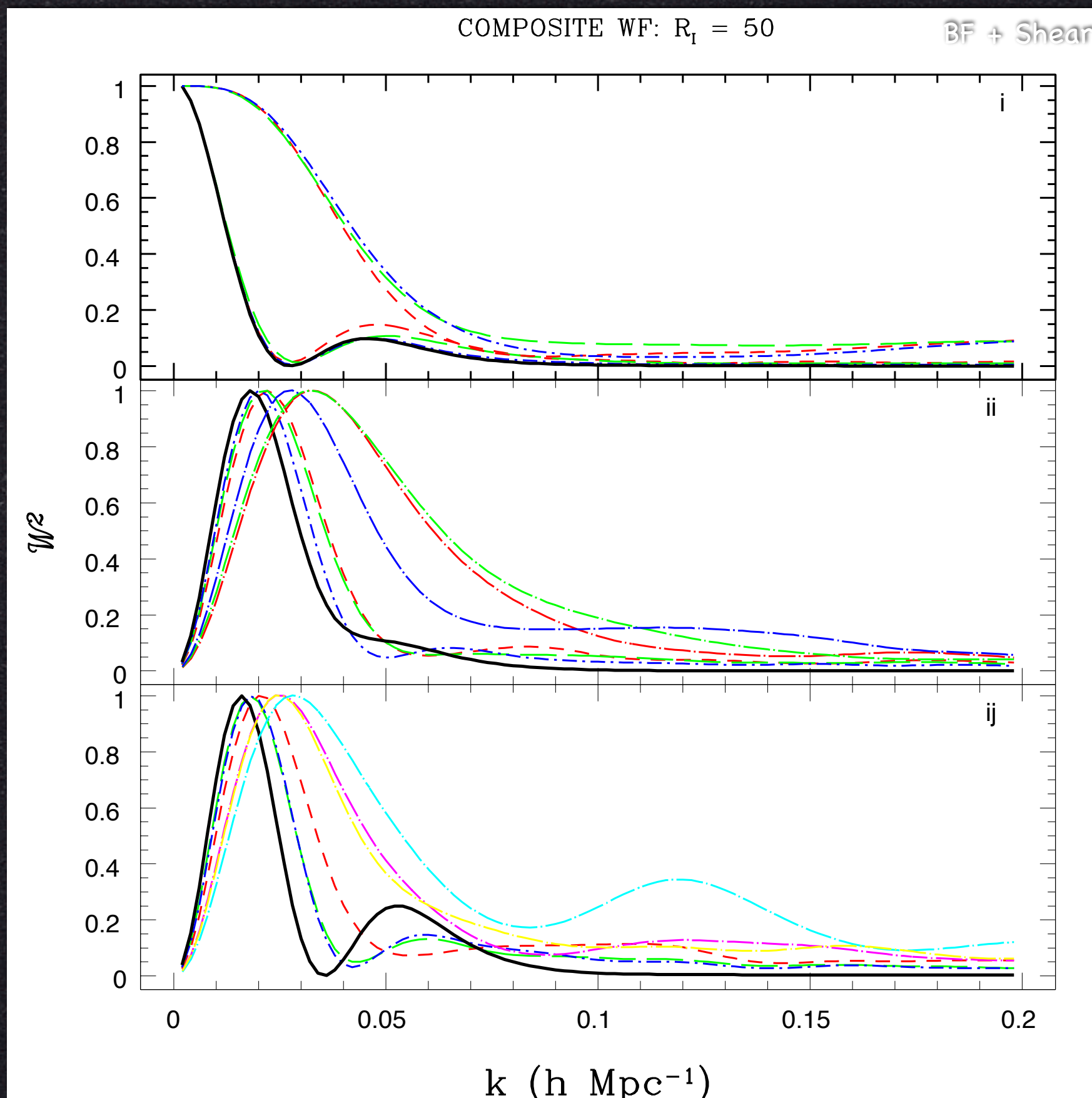


Peculiar Velocity Surveys

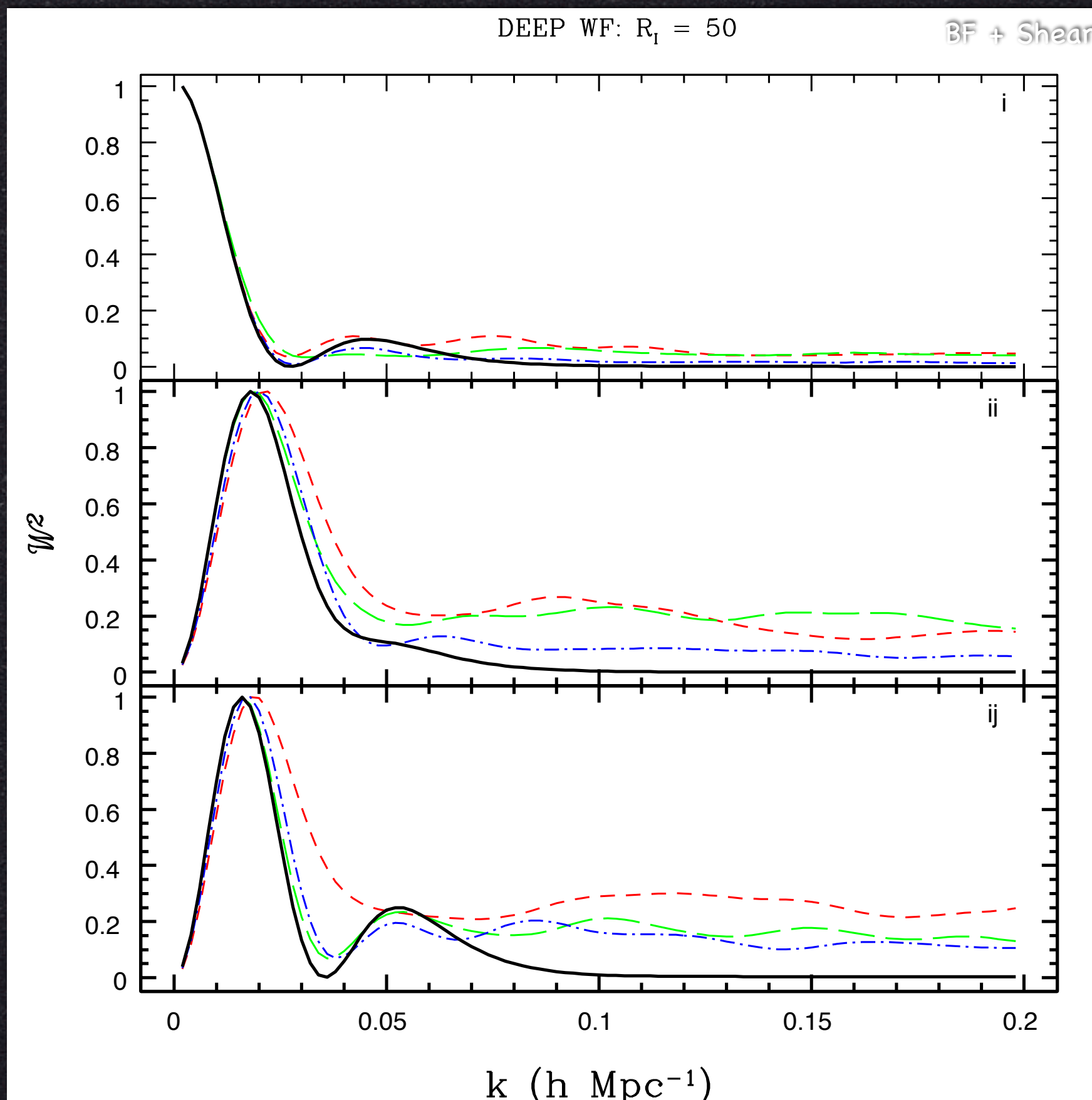
COMPOSITE (4481 Galaxies, Groups & Clusters)



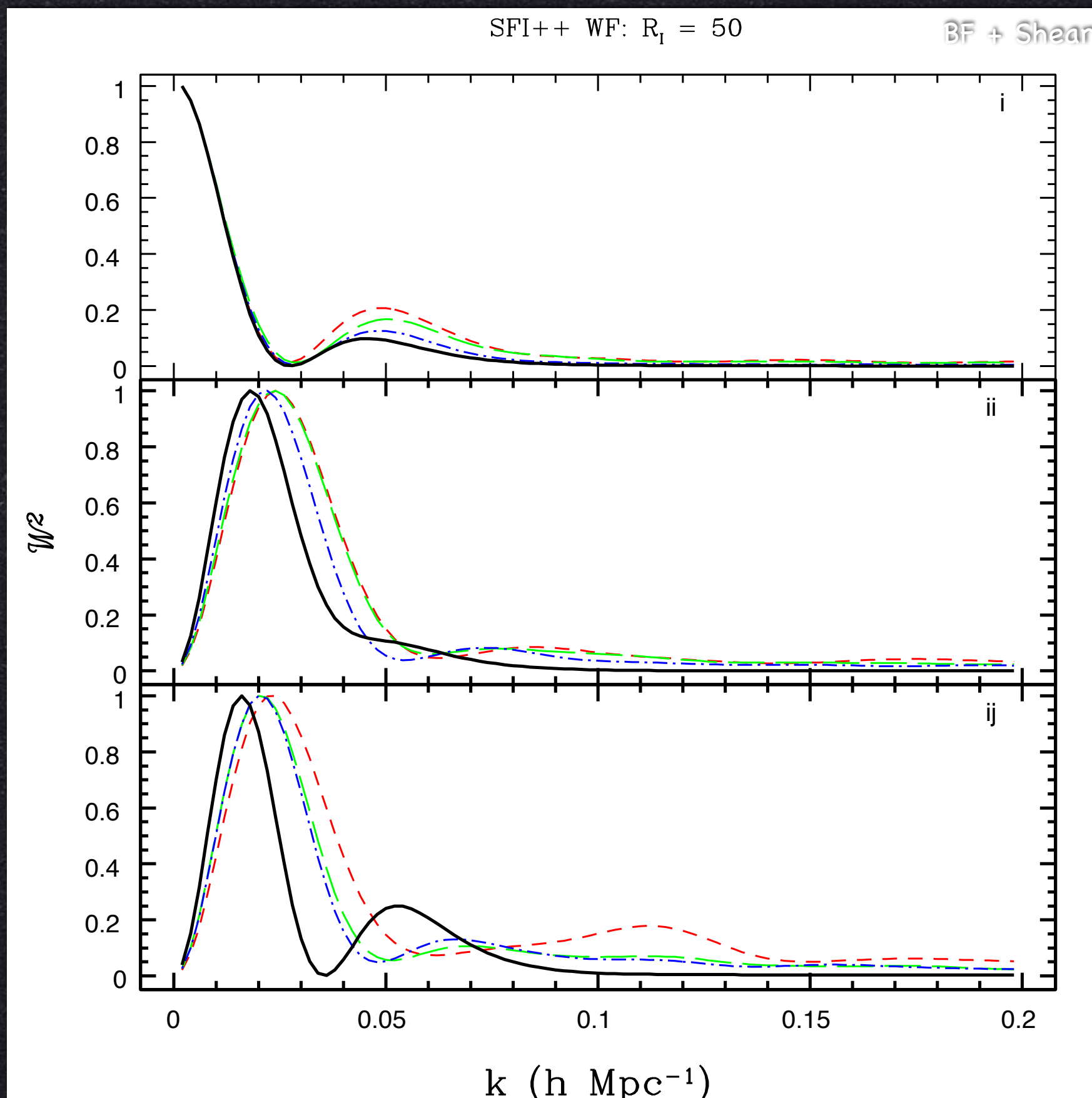
Window Function Design



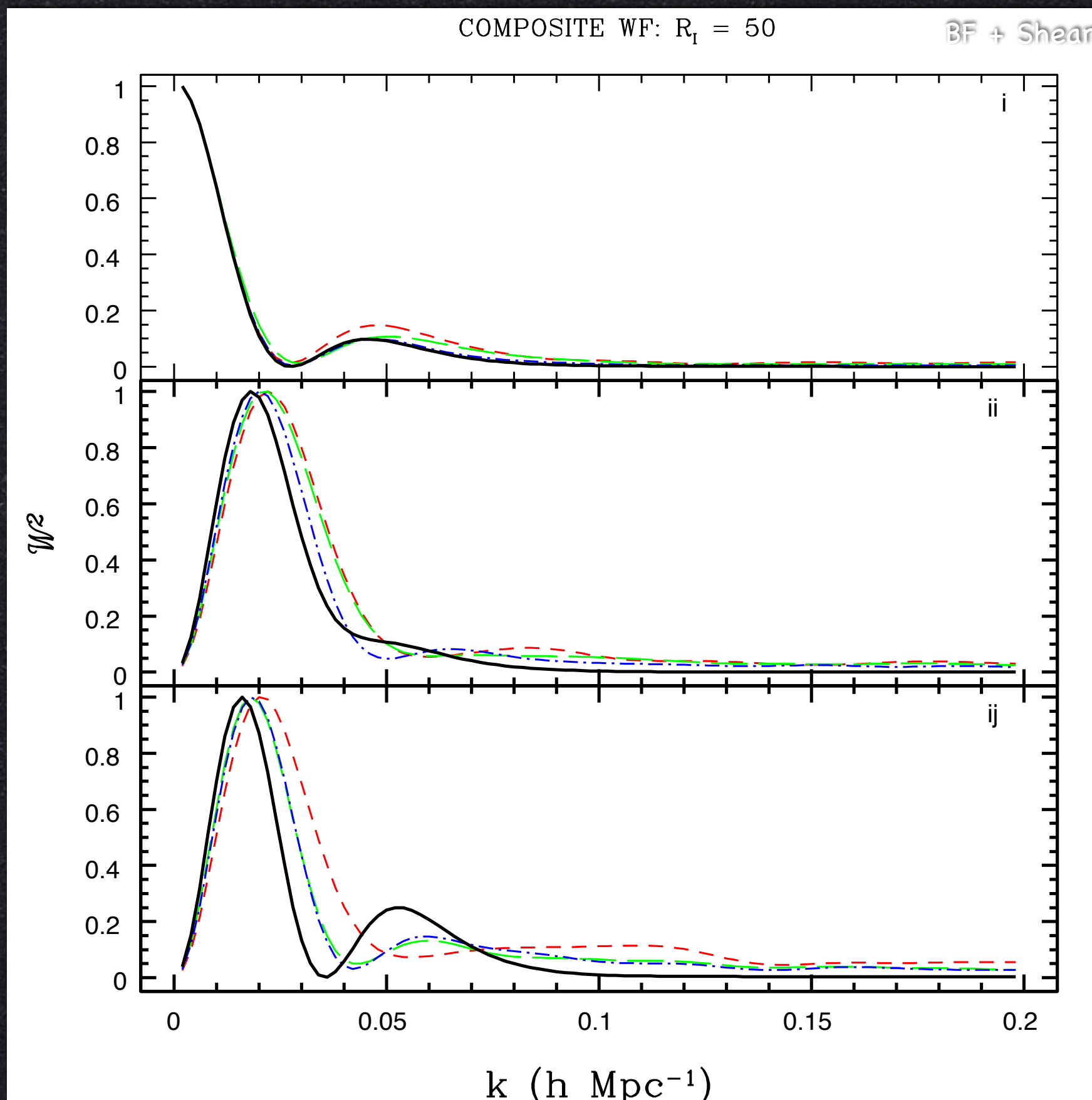
Window Function Design

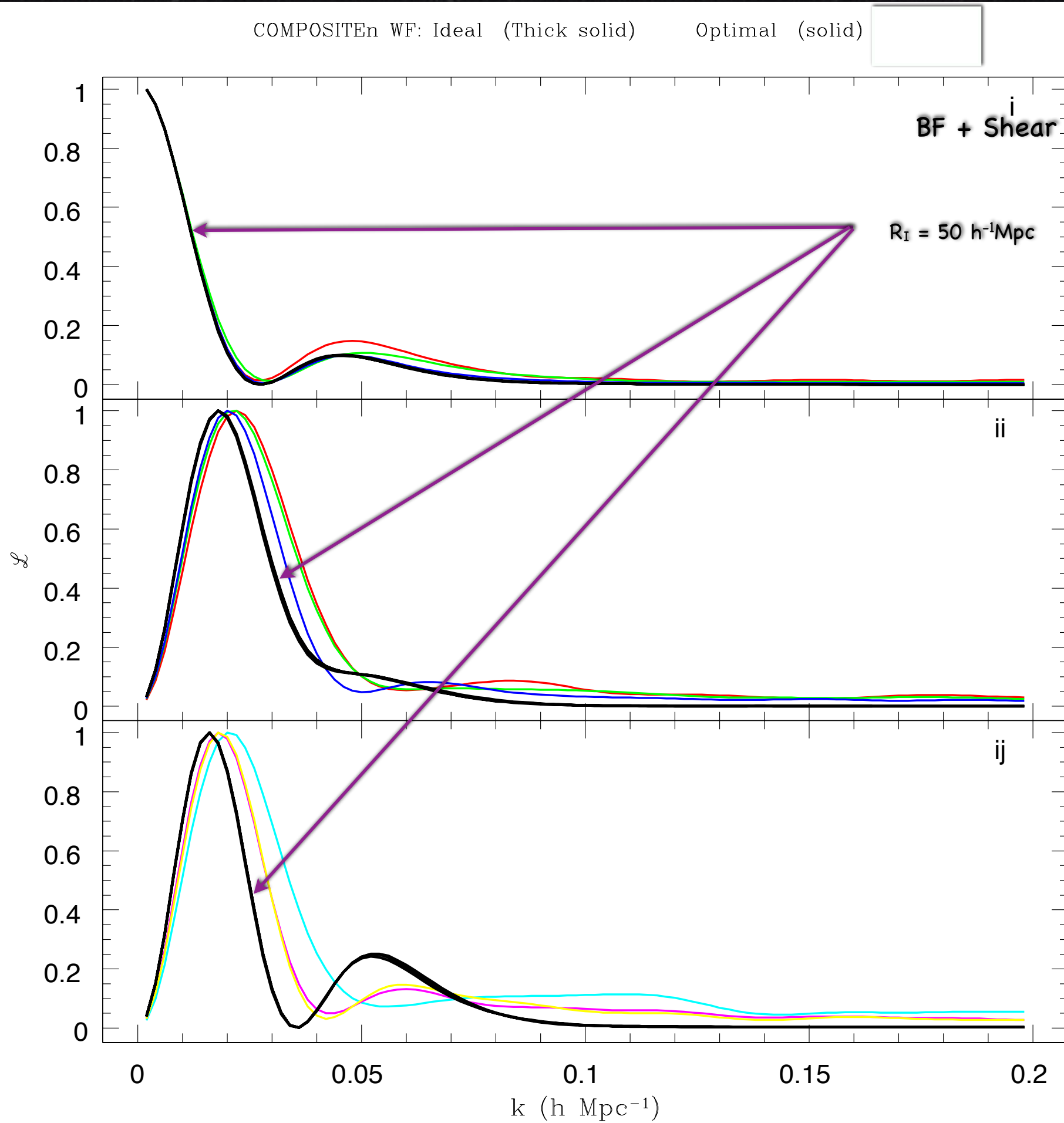


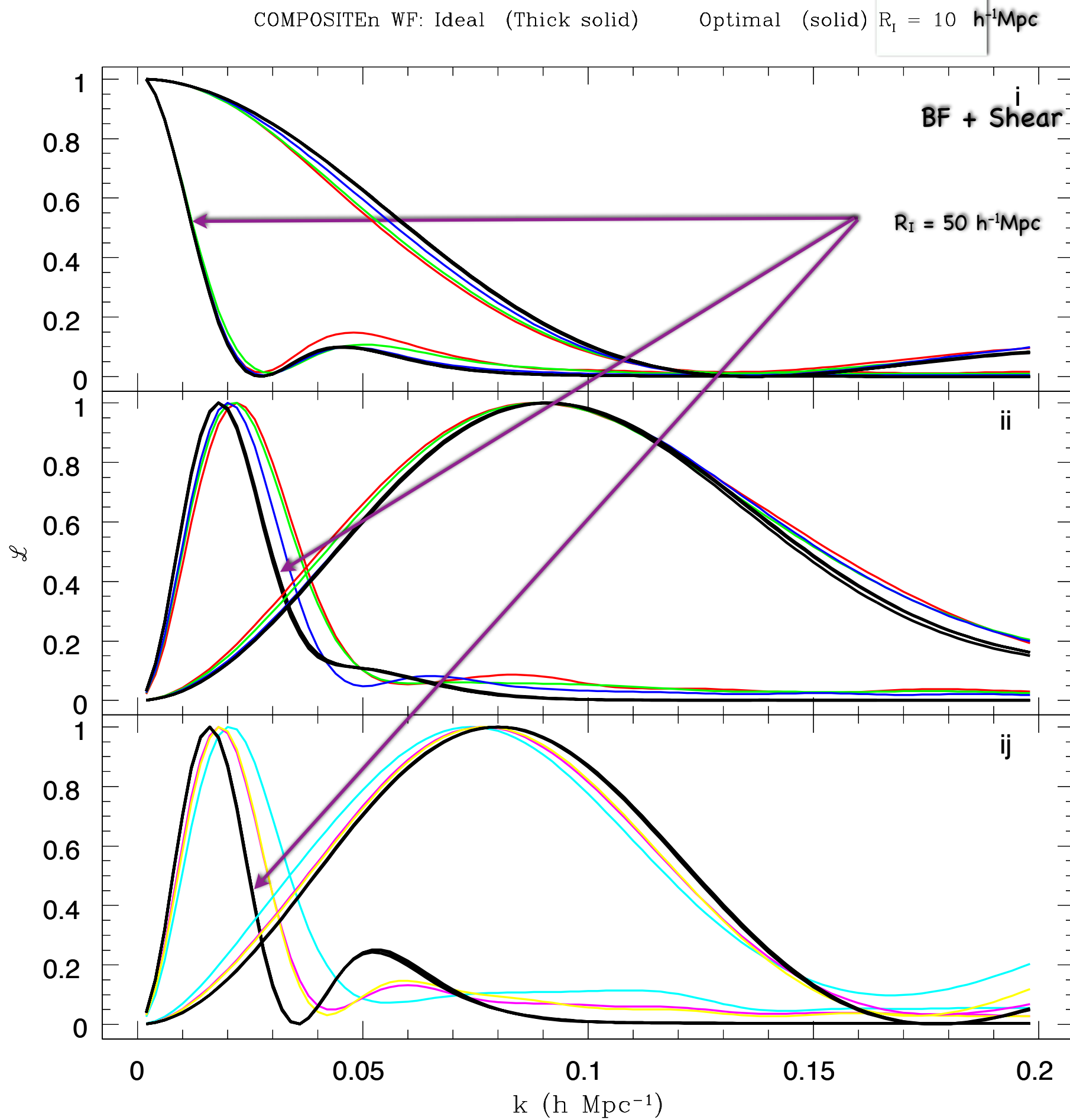
Window Function Design

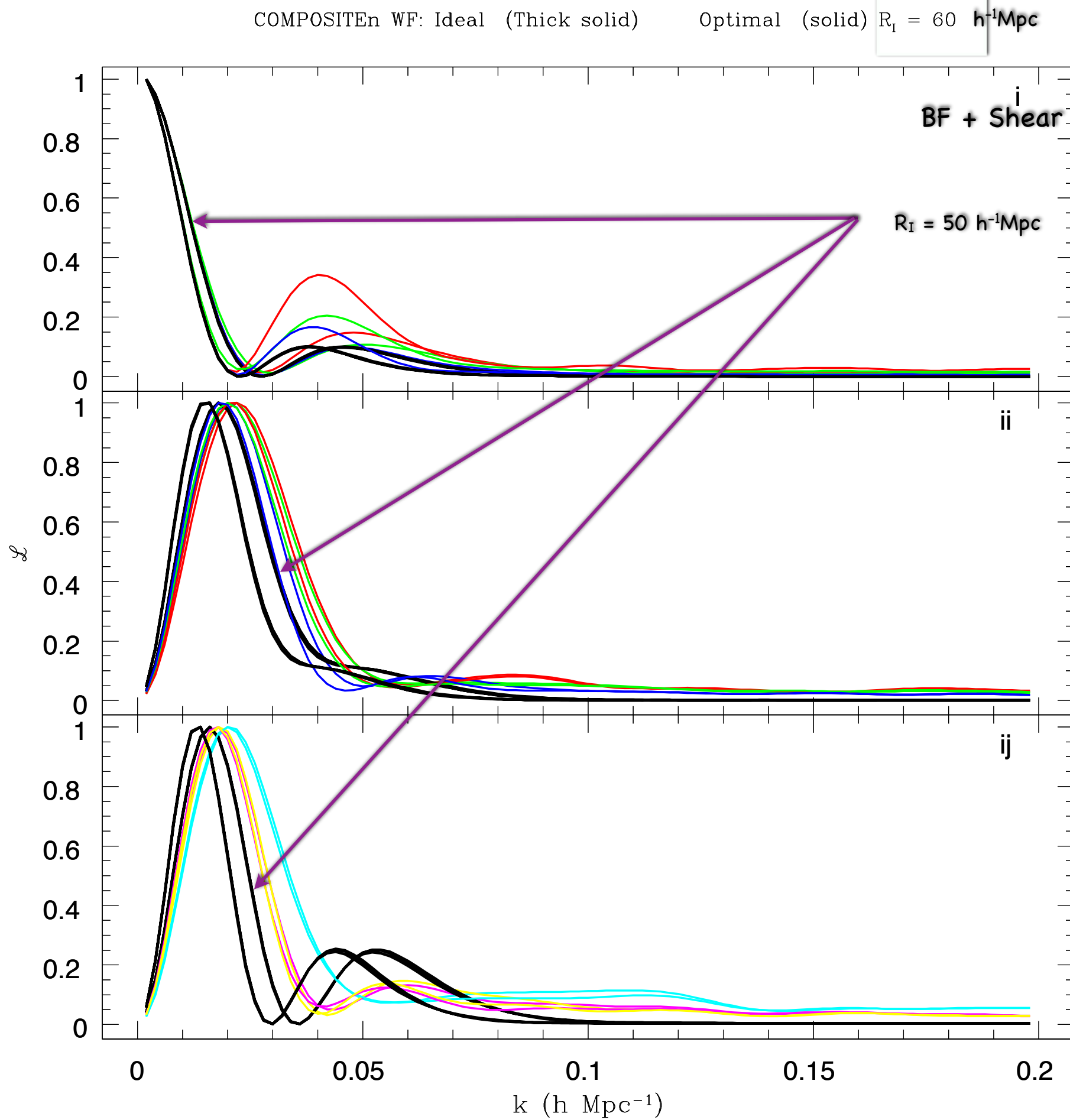


Window Function Design

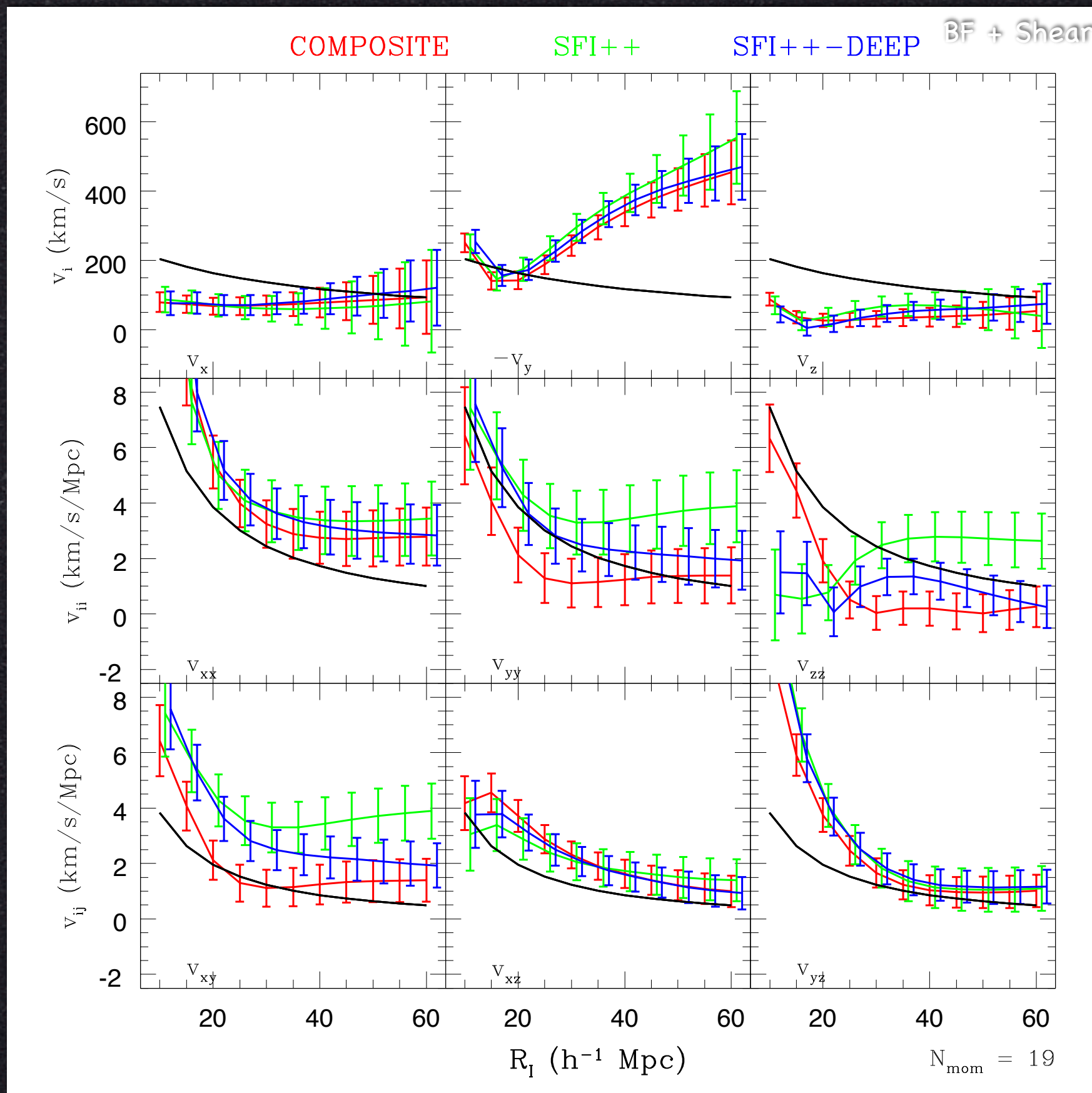




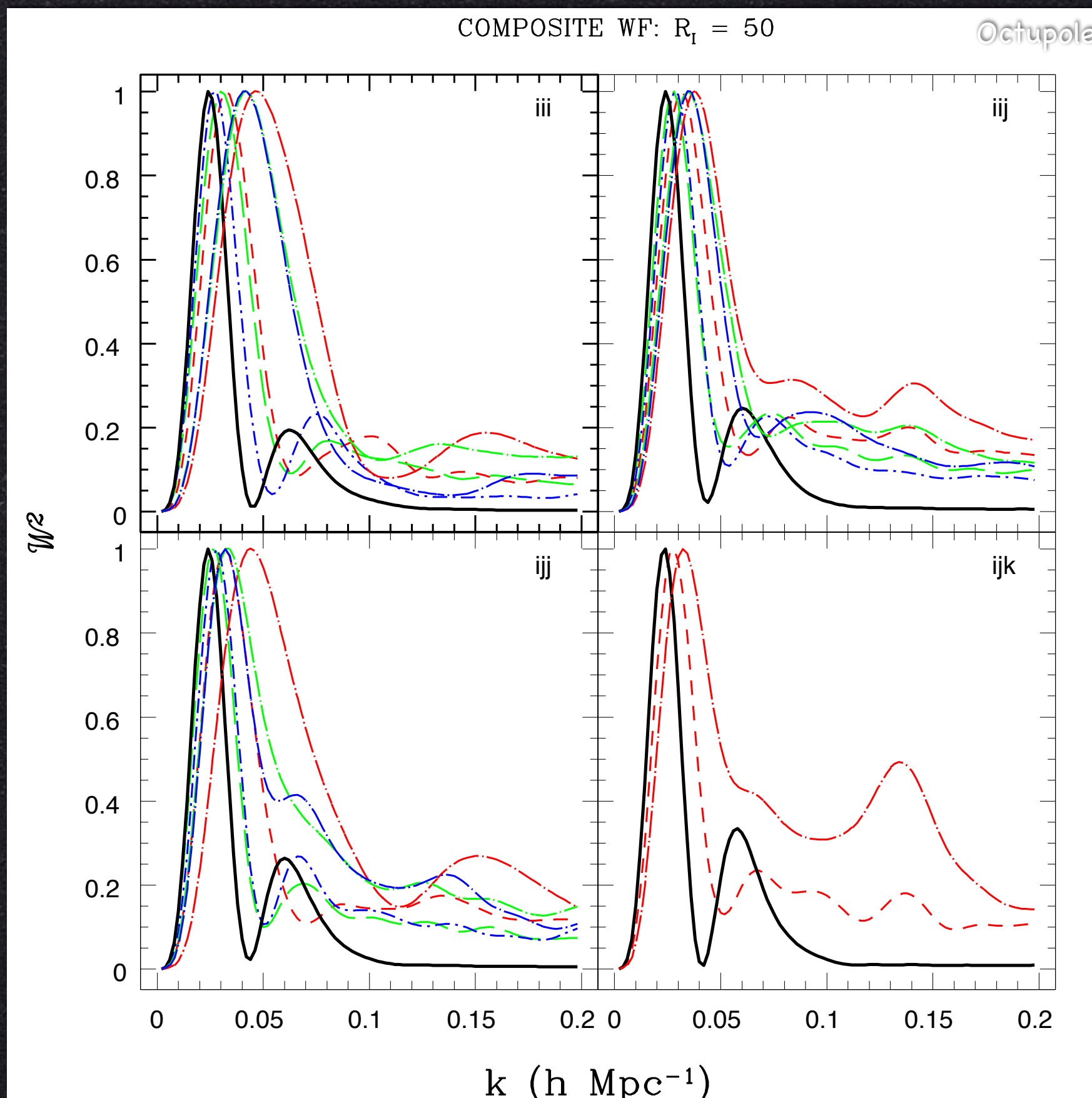




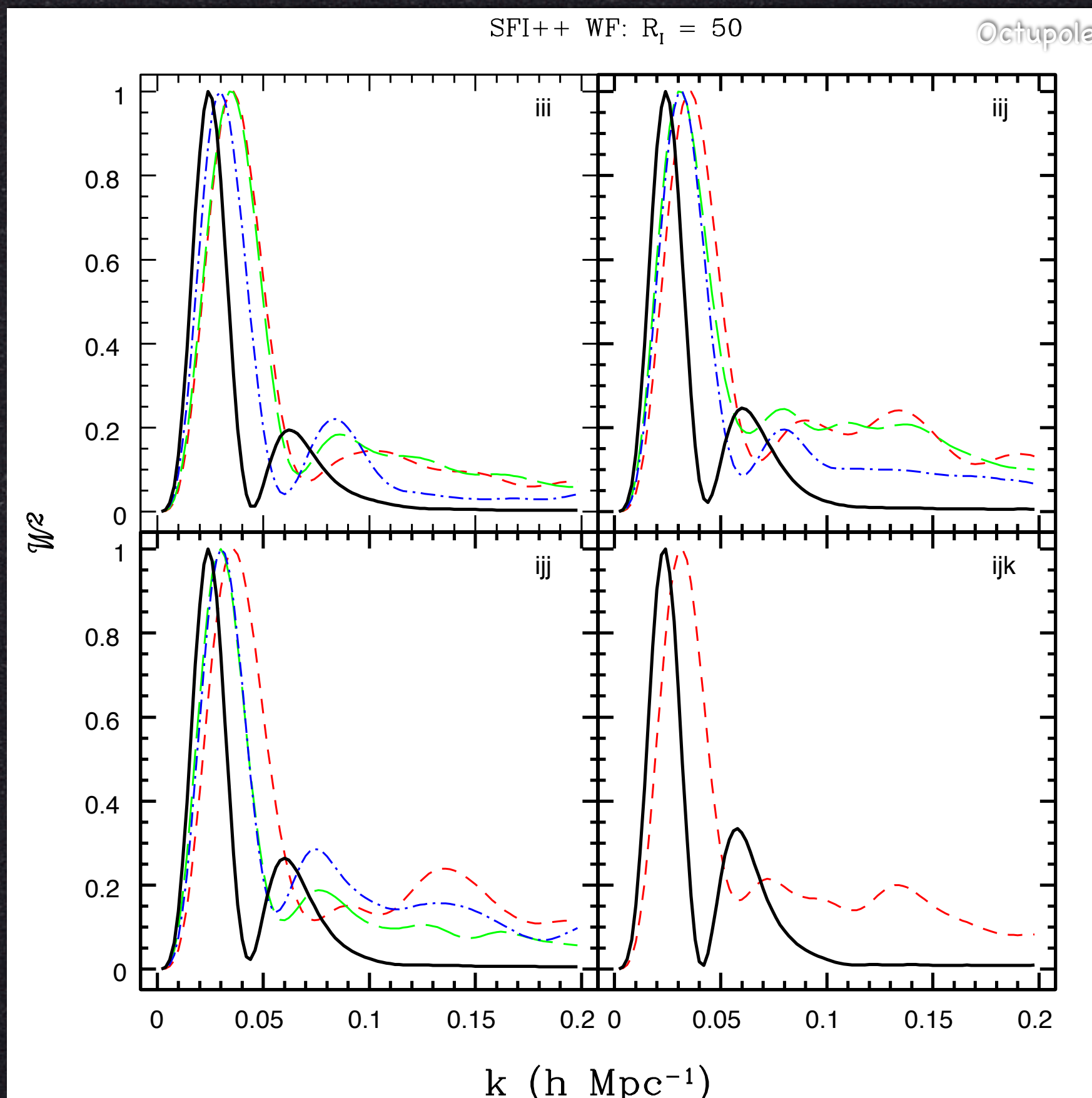
Comparing Surveys



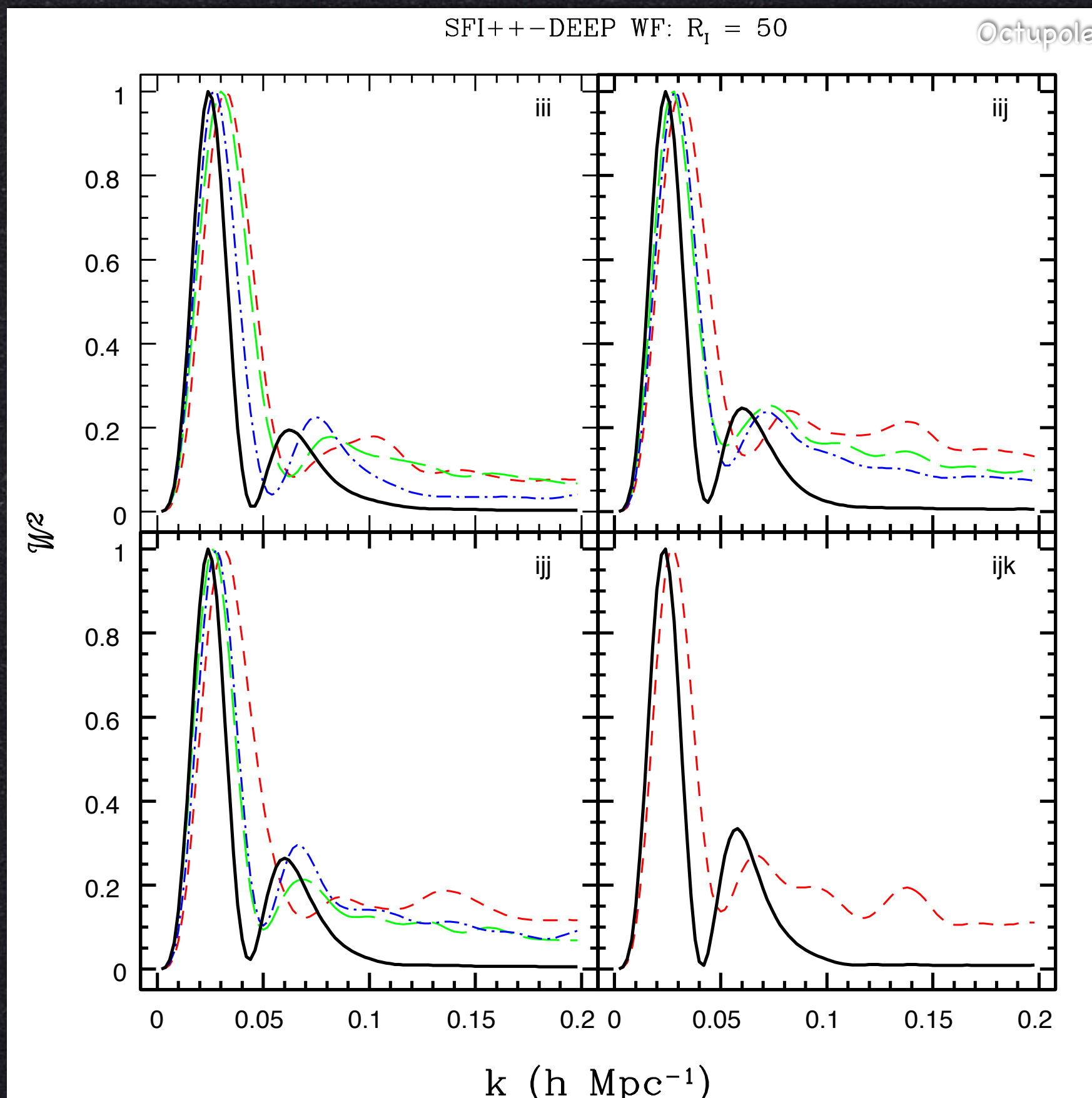
Window Function Design



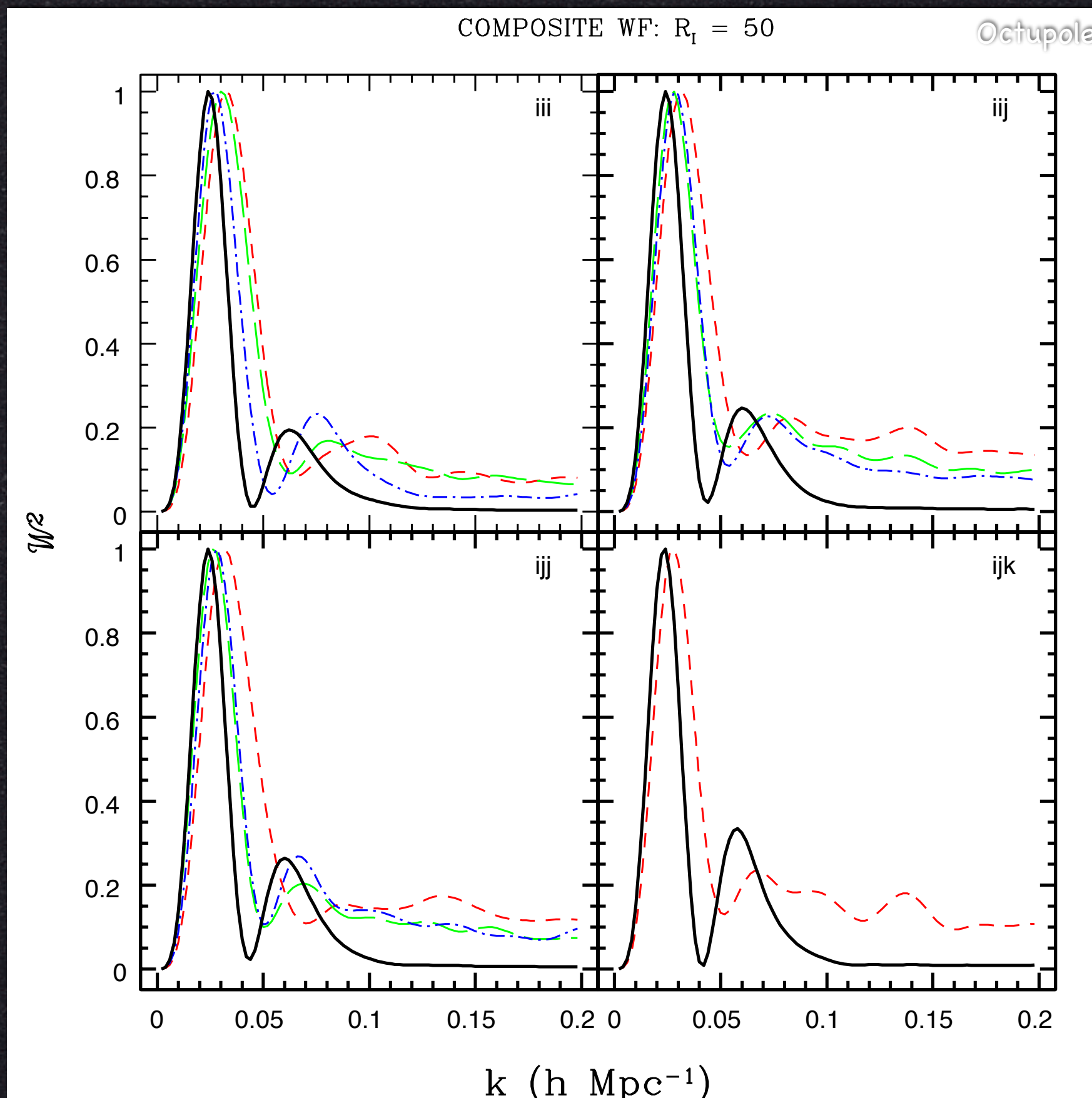
Window Function Design

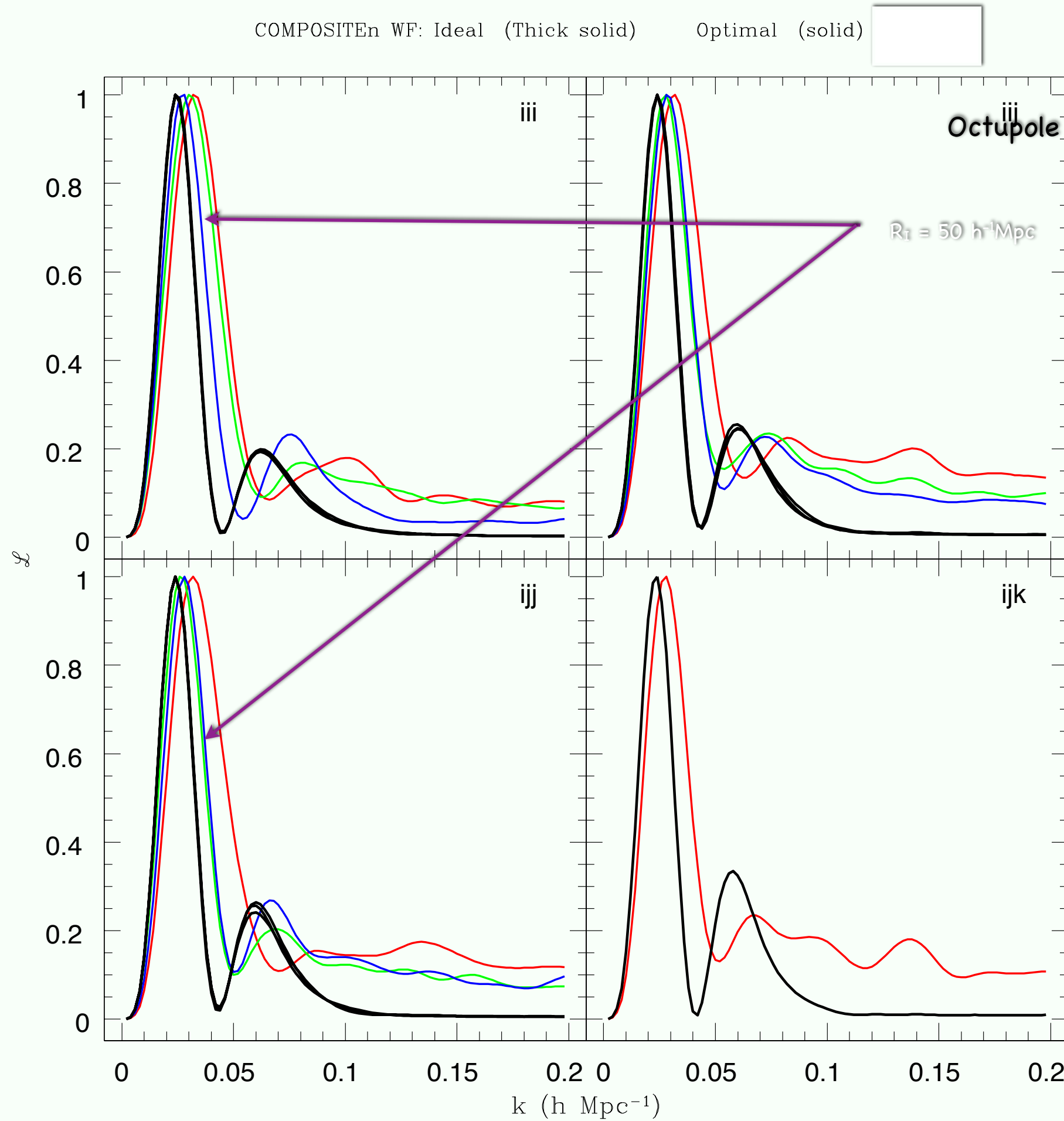


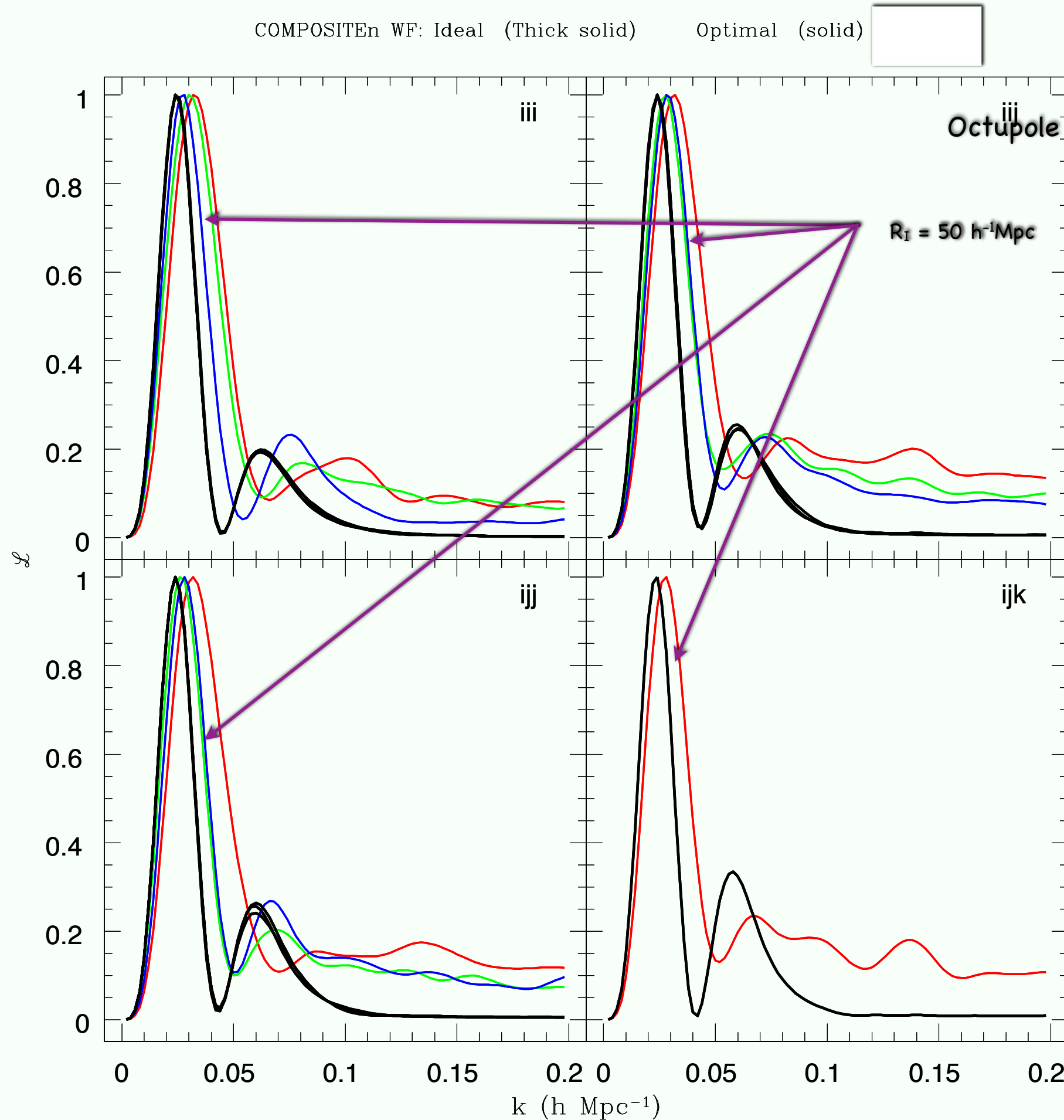
Window Function Design

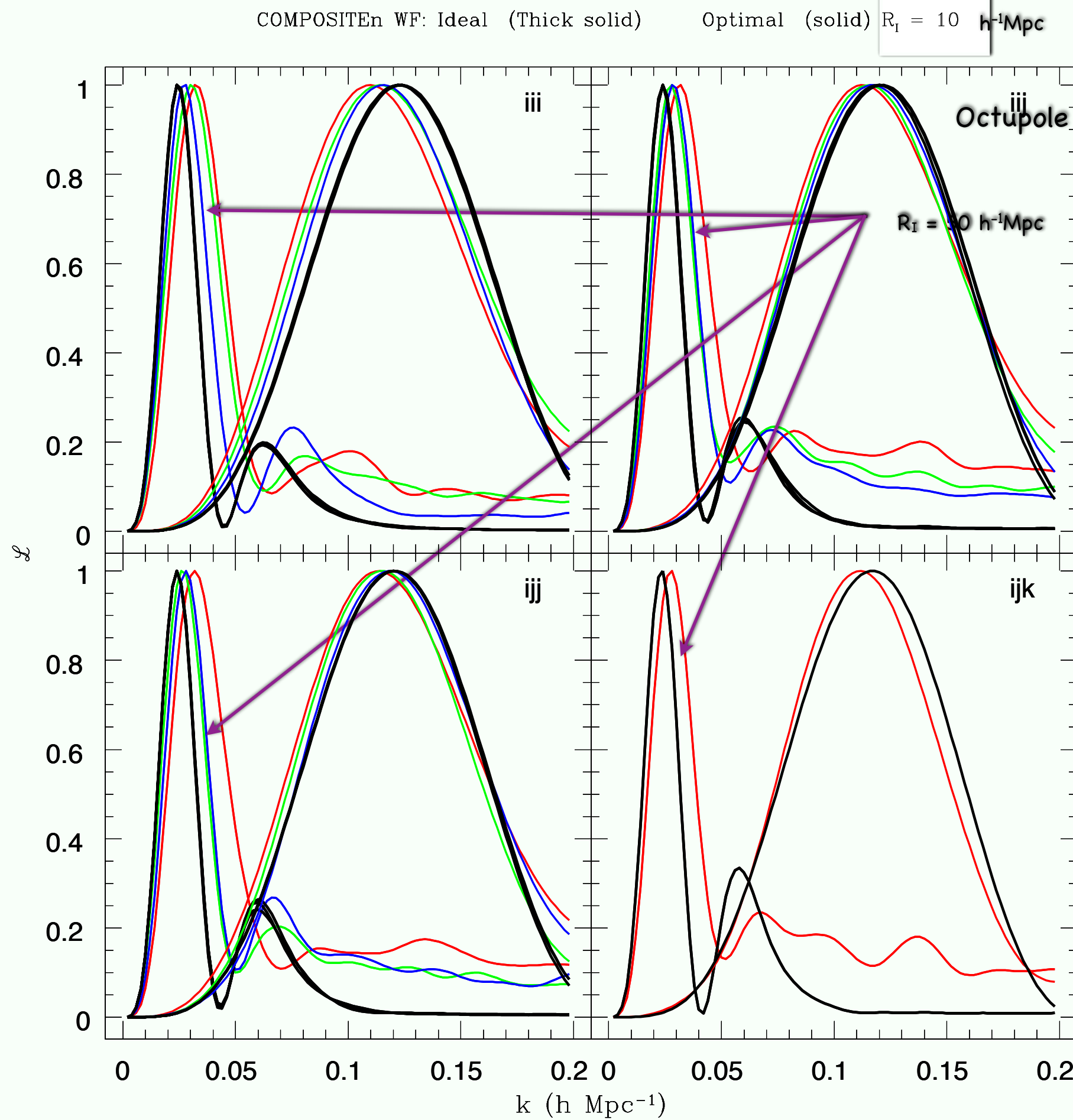


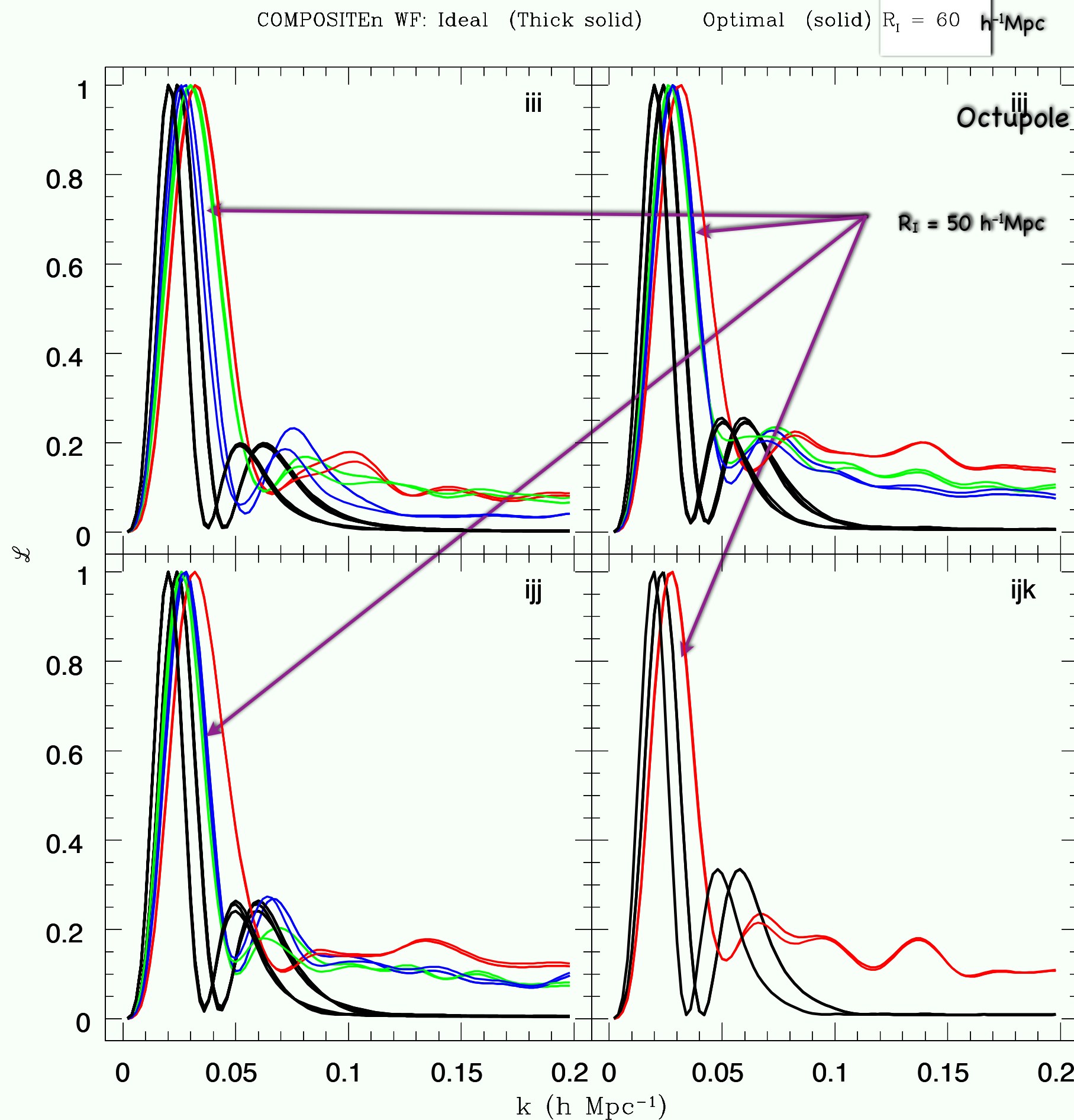
Window Function Design

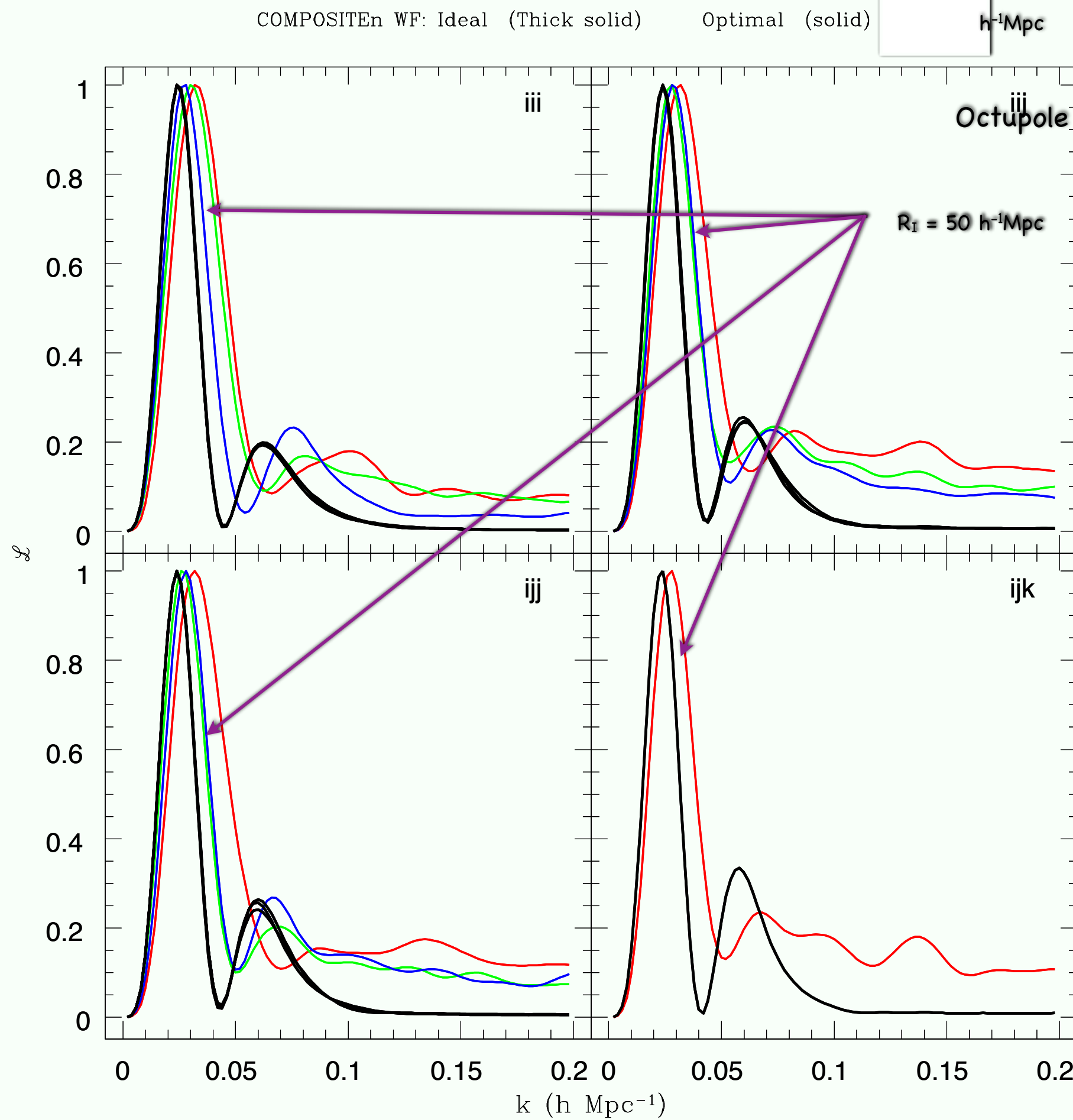




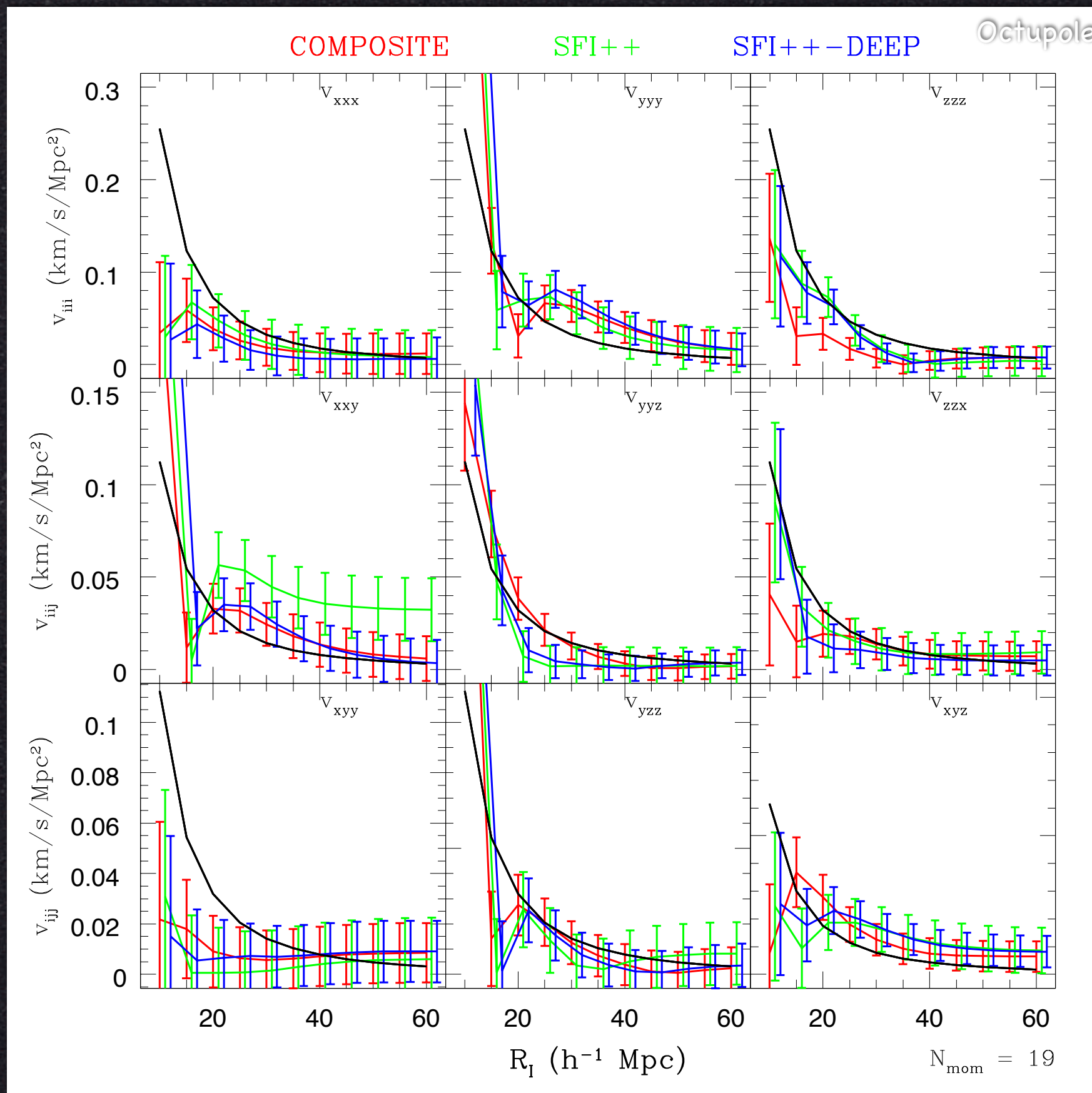








Comparing Surveys



Moments and correlation coefficients

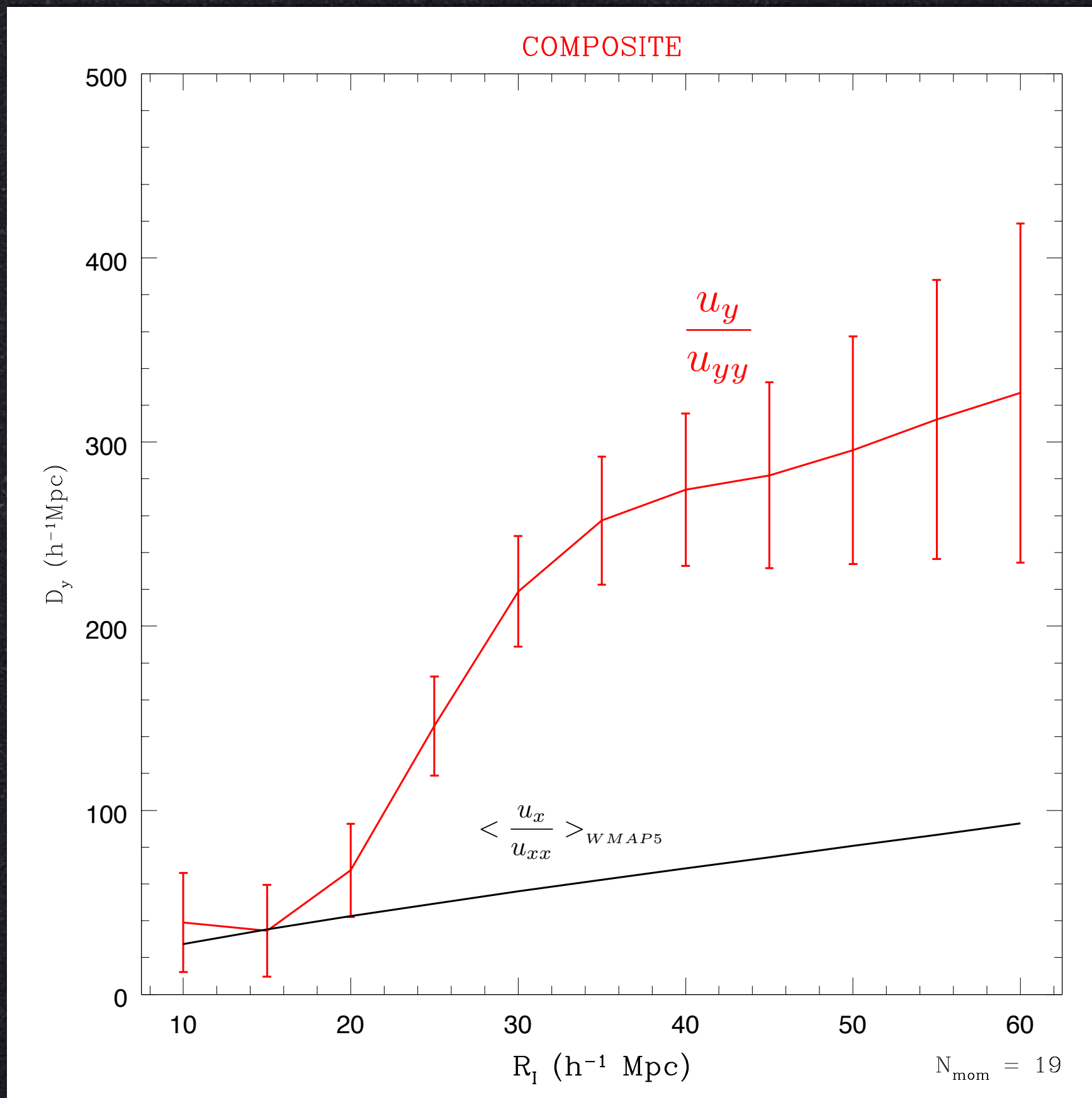
	COMPOSITE		SFI++-DEEP		SFI++		DEEP	
x	86.5 ± 68.8	0.74	104.7 ± 71.0	0.72	69.0 ± 95.7	0.64	192.7 ± 115.6	0.51
y	-404.9 ± 61.8	0.77	-430.3 ± 63.8	0.75	-473.6 ± 87.2	0.67	-320.7 ± 106.0	0.51
z	42.8 ± 37.7	0.89	64.9 ± 38.7	0.88	57.7 ± 59.3	0.80	62.0 ± 55.8	0.76
xx	2.73 ± 1.01	0.69	2.94 ± 1.05	0.68	3.36 ± 1.29	0.62	2.19 ± 1.76	0.47
yy	1.37 ± 0.98	0.69	2.07 ± 1.02	0.68	3.72 ± 1.27	0.63	-0.19 ± 1.79	0.42
zz	-0.03 ± 0.68	0.80	0.68 ± 0.72	0.79	2.72 ± 0.96	0.71	-0.72 ± 1.04	0.67
xy	0.13 ± 0.76	0.51	-0.01 ± 0.79	0.50	-0.71 ± 0.98	0.42	0.27 ± 1.29	0.31
yz	-0.95 ± 0.57	0.63	-1.14 ± 0.59	0.62	-1.05 ± 0.78	0.52	-0.71 ± 0.94	0.40
zx	1.22 ± 0.54	0.66	1.14 ± 0.56	0.65	1.50 ± 0.74	0.56	0.98 ± 0.84	0.47
xxx	$-1.2e-2 \pm 2.2e-2$	0.38	$-5.8e-3 \pm 2.3e-2$	0.37	$-9.3e-3 \pm 2.9e-2$	0.31	$1.0e-2 \pm 3.6e-2$	0.25
yyy	$-2.4e-2 \pm 1.7e-2$	0.41	$-2.3e-2 \pm 1.8e-2$	0.40	$-1.9e-2 \pm 2.4e-2$	0.34	$-2.2e-2 \pm 2.7e-2$	0.24
zzz	$-7.2e-3 \pm 1.1e-2$	0.61	$-7.7e-3 \pm 1.1e-2$	0.60	$-3.3e-3 \pm 1.6e-2$	0.48	$-2.5e-3 \pm 1.6e-2$	0.47
xyy	$-8.2e-3 \pm 1.2e-2$	0.30	$-5.7e-3 \pm 1.3e-2$	0.30	$-3.3e-2 \pm 1.7e-2$	0.23	$2.0e-2 \pm 1.9e-2$	0.20
yzz	$5.8e-4 \pm 6.6e-3$	0.44	$2.8e-3 \pm 6.7e-3$	0.44	$-1.8e-3 \pm 1.0e-2$	0.33	$8.9e-3 \pm 9.6e-3$	0.30
zxx	$7.3e-3 \pm 7.8e-3$	0.45	$4.9e-3 \pm 8.1e-3$	0.45	$8.7e-3 \pm 1.1e-2$	0.34	$-2.1e-3 \pm 1.2e-2$	0.34
xyy	$8.3e-3 \pm 1.2e-2$	0.29	$9.0e-3 \pm 1.2e-2$	0.28	$5.7e-3 \pm 1.6e-2$	0.24	$2.2e-2 \pm 1.9e-2$	0.16
yyz	$6.3e-4 \pm 8.3e-3$	0.40	$2.2e-3 \pm 8.5e-3$	0.40	$7.7e-3 \pm 1.2e-2$	0.28	$-2.5e-3 \pm 1.2e-2$	0.30
zzx	$1.2e-2 \pm 7.6e-3$	0.46	$9.9e-3 \pm 7.8e-3$	0.46	$-2.5e-3 \pm 1.1e-2$	0.35	$1.6e-2 \pm 1.1e-2$	0.34
xyz	$6.6e-3 \pm 5.5e-3$	0.34	$8.7e-3 \pm 5.6e-3$	0.34	$9.3e-3 \pm 8.2e-3$	0.25	$4.9e-3 \pm 8.2e-3$	0.22

The total observed $P(>\chi^2)$ in percent for $N_{\text{MOM}} = 3, 9$ and 19 for $R_I = 50 \text{ h}^{-1} \text{ Mpc}$, and the WMAP5 central parameters $\Omega_m = 0.258$ and $\sigma_8 = 0.796$.

	$N_{\text{MOM}} = 3$	$N_{\text{MOM}} = 9$			$N_{\text{MOM}} = 19$			
	BF	Total	BF	shear	Total	BF	shear	octupole
COMPOSITE	1.89	6.01	1.81	41.76	17.00	0.50	52.60	78.33
SFI++-DEEP	0.92	2.80	0.85	33.21	13.67	0.20	39.47	86.37
SFI++	3.11	1.73	3.22	7.70	16.19	0.22	11.22	89.38
DEEP	6.02	30.41	6.29	82.62	55.54	3.18	91.22	81.61

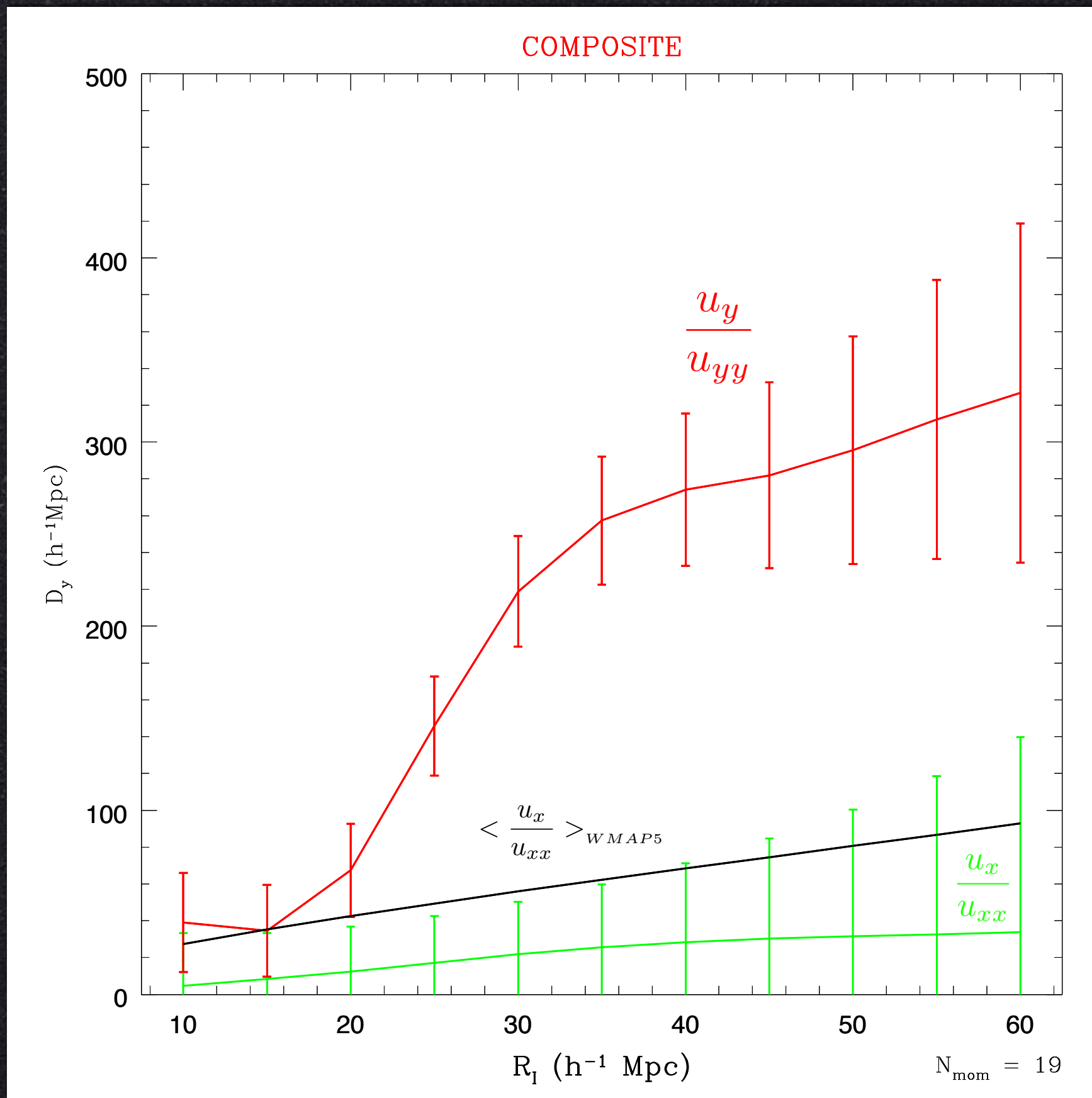
Sources of the Flow

Work in progress

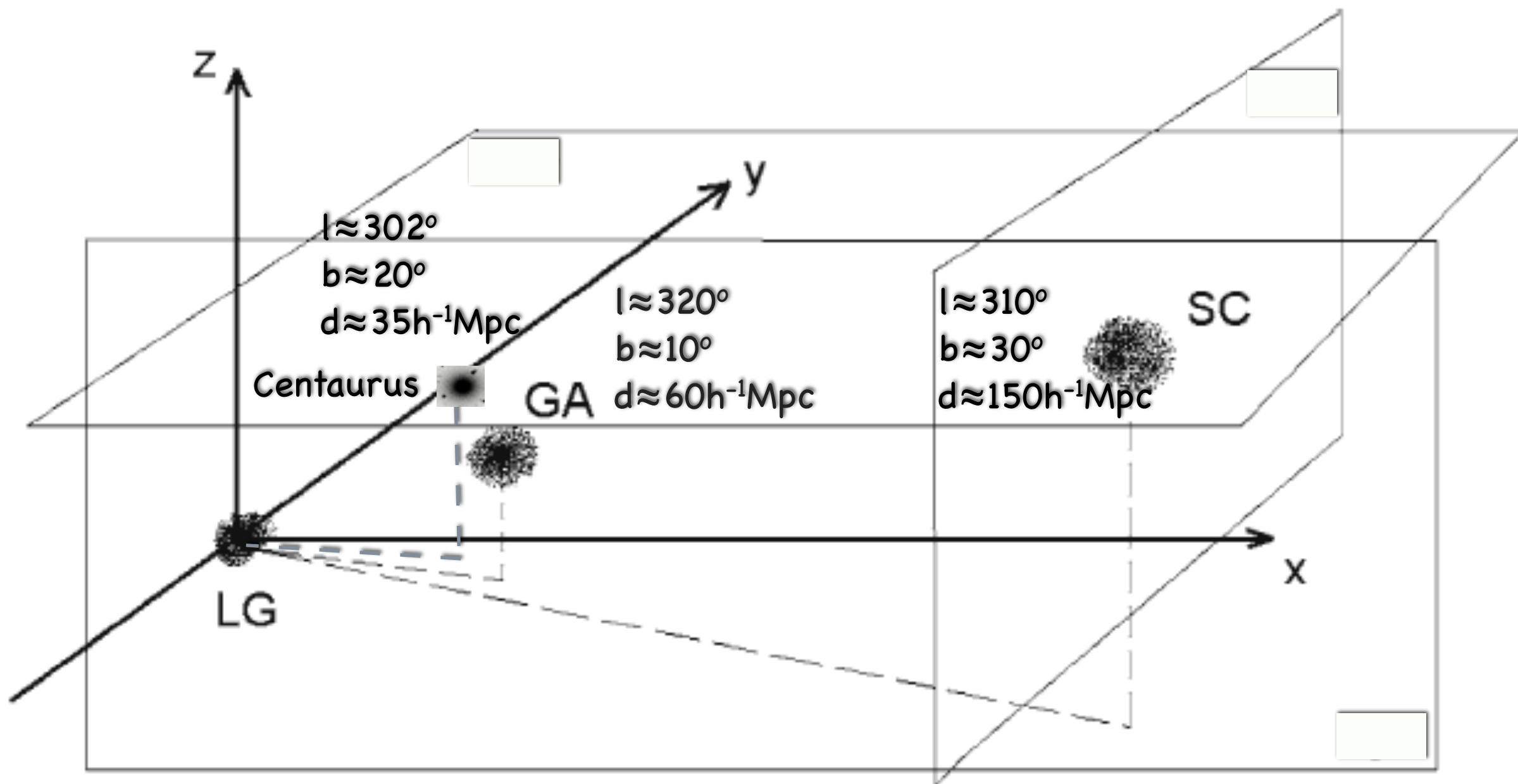


Sources of the Flow

Work in progress

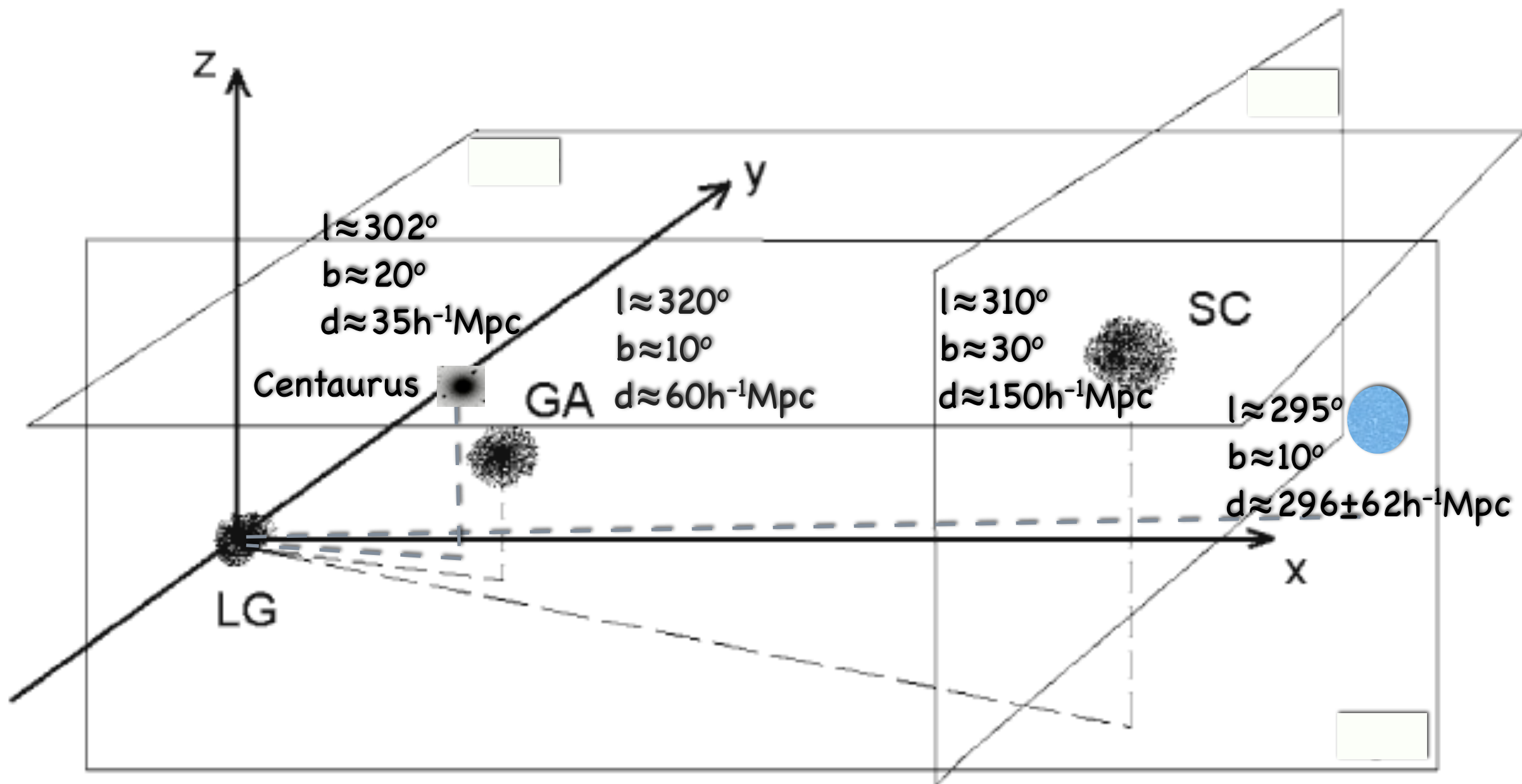


Is there an attractor?



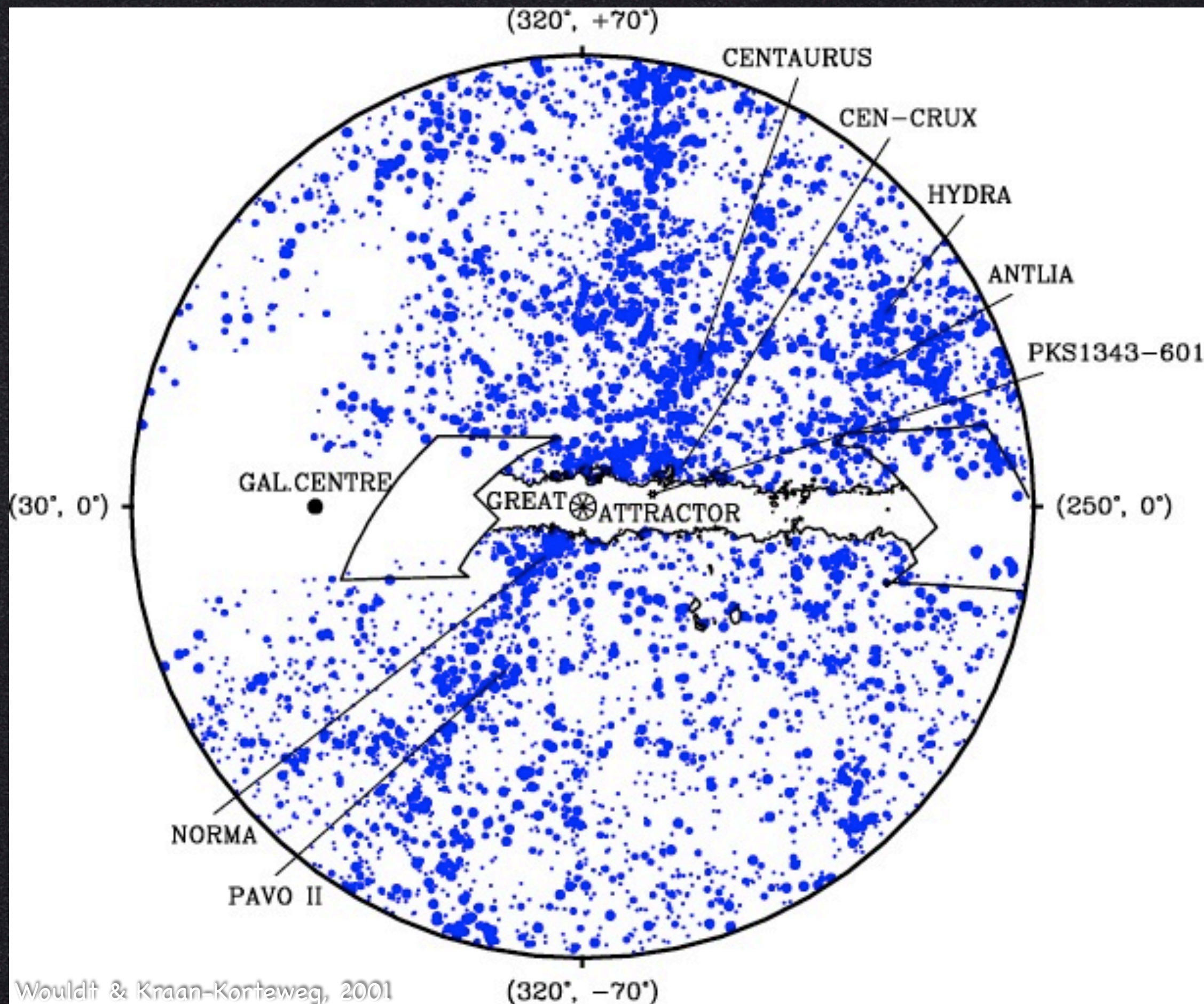
Bolejko & Hellaby 2008

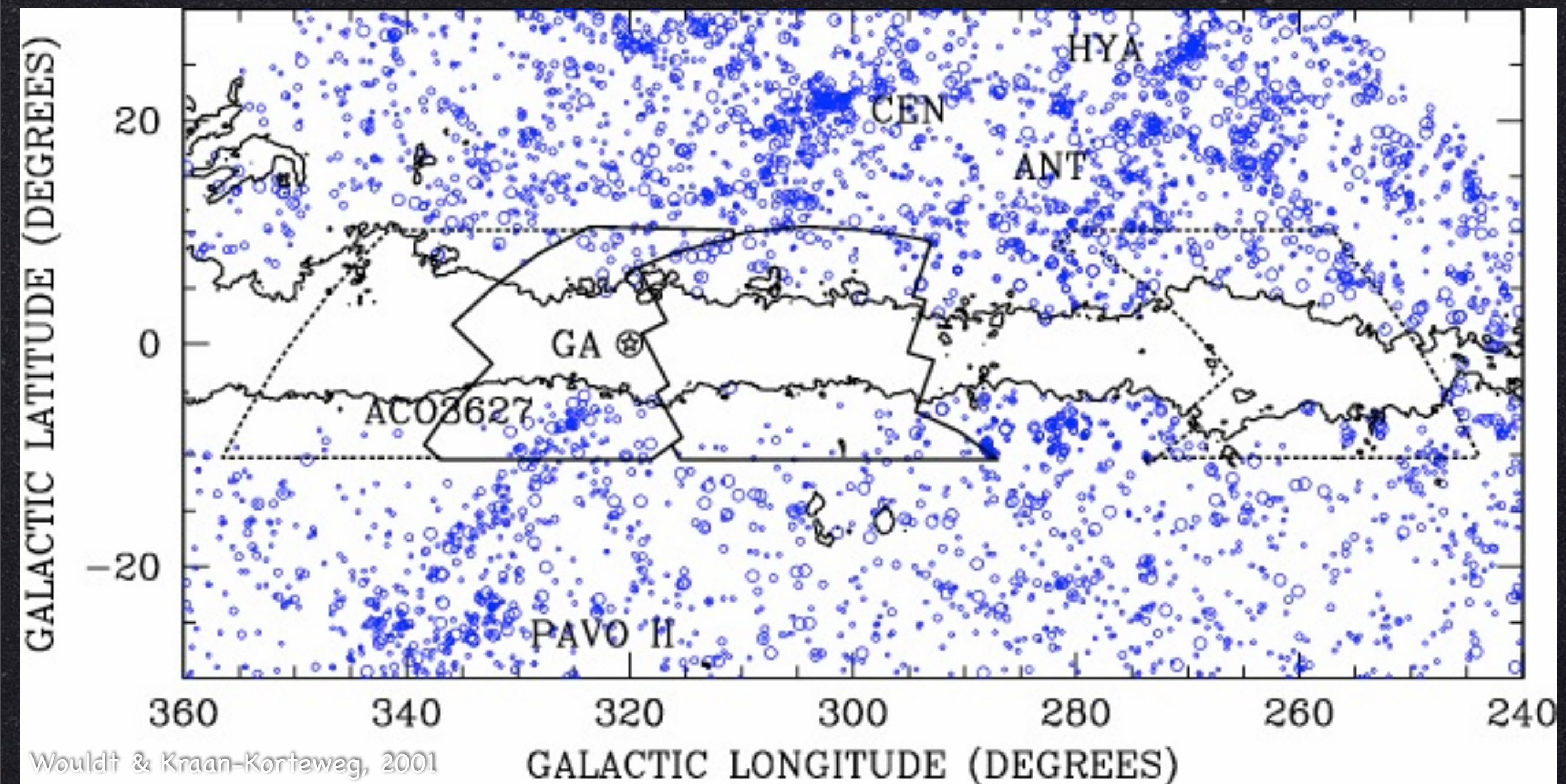
Is there an attractor?

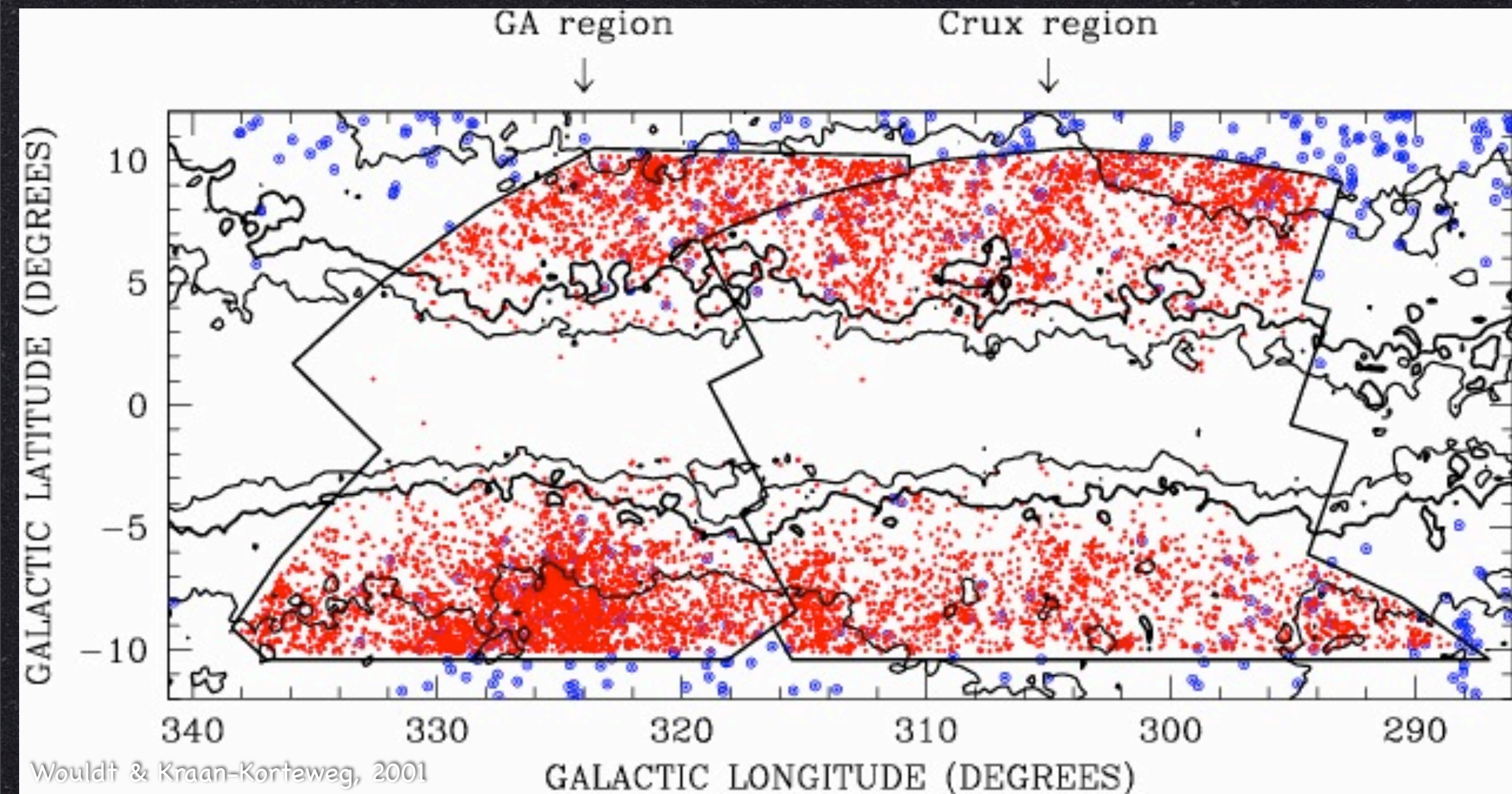


Bolejko & Hellaby 2008

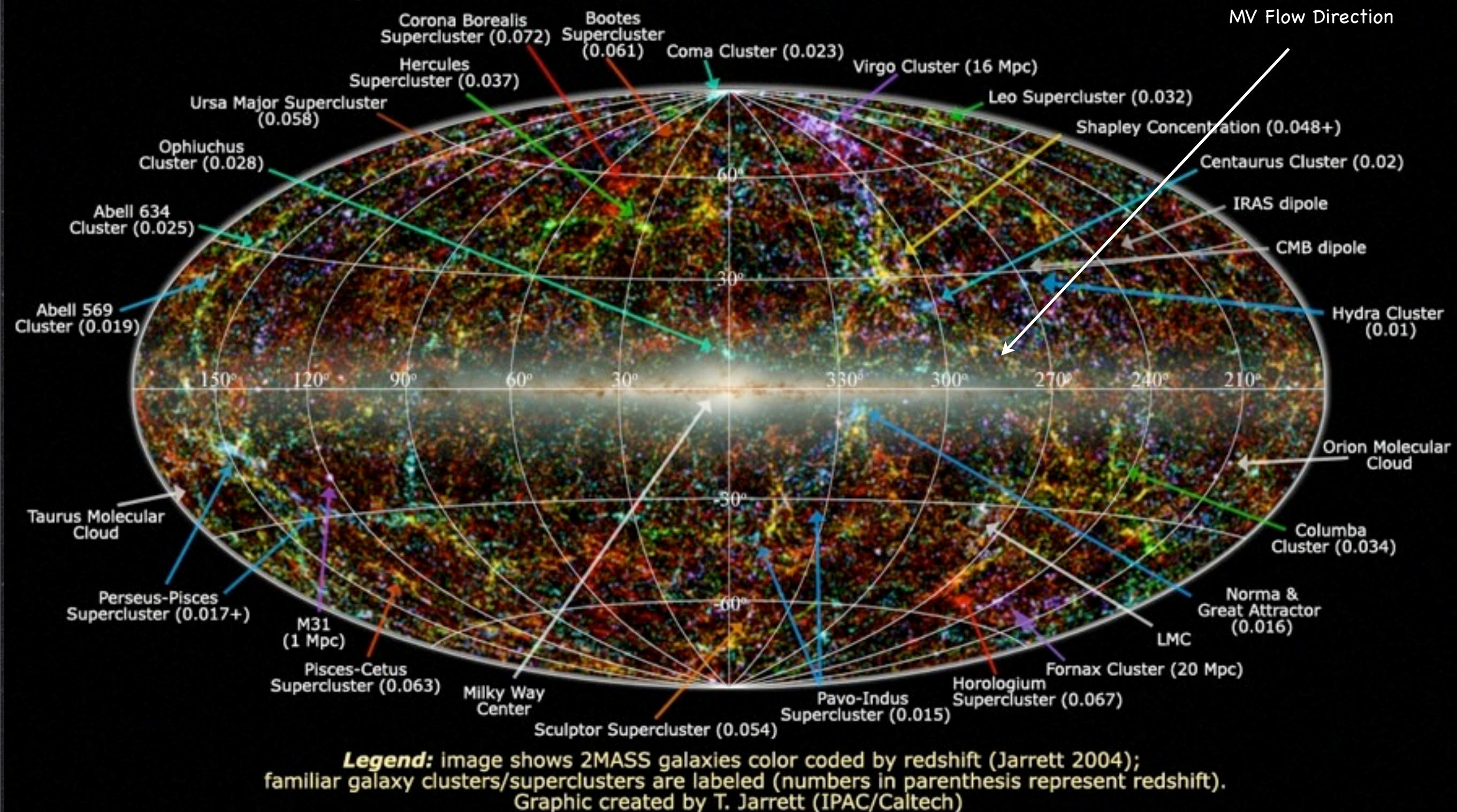
Is there an attractor?

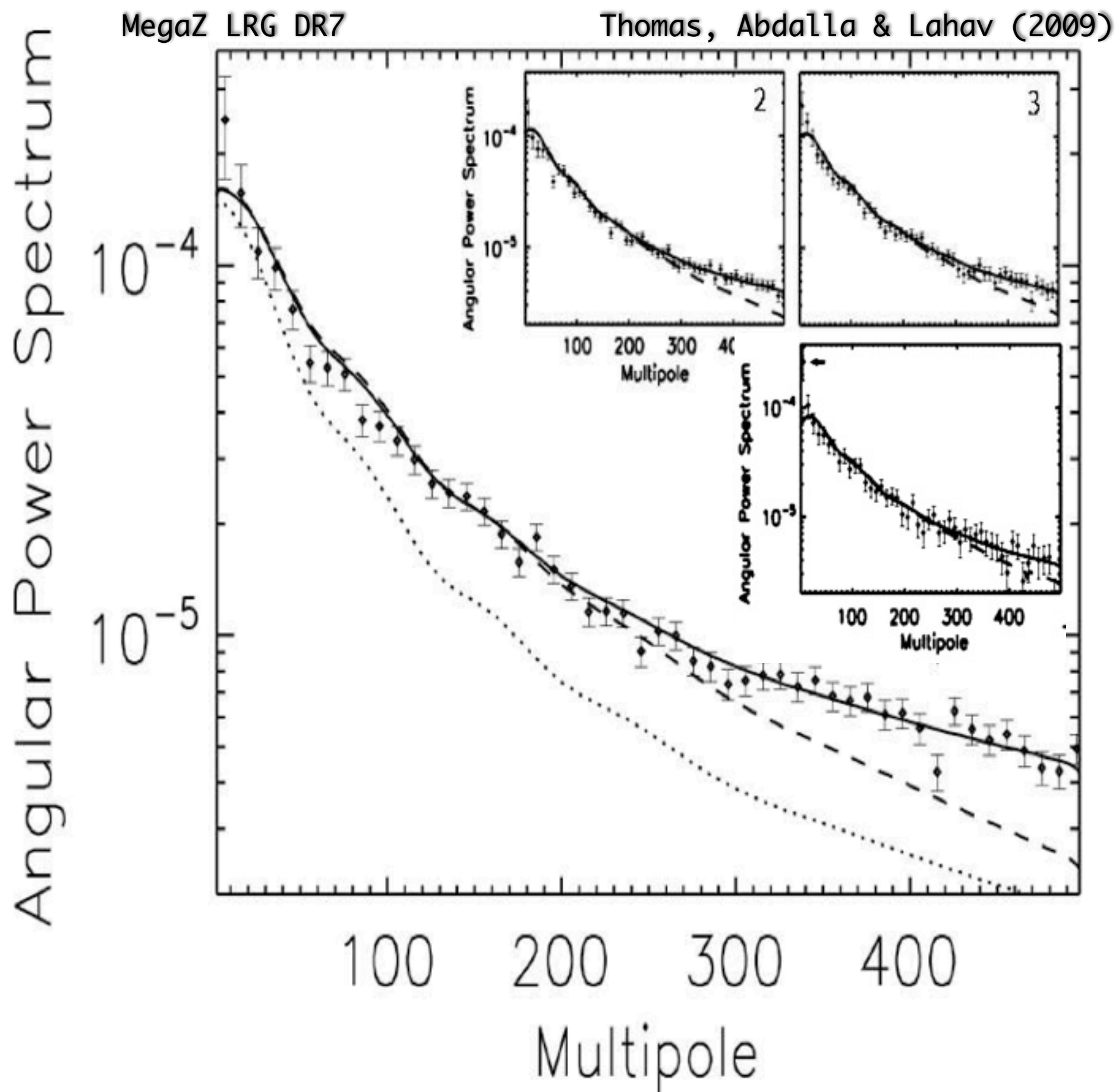


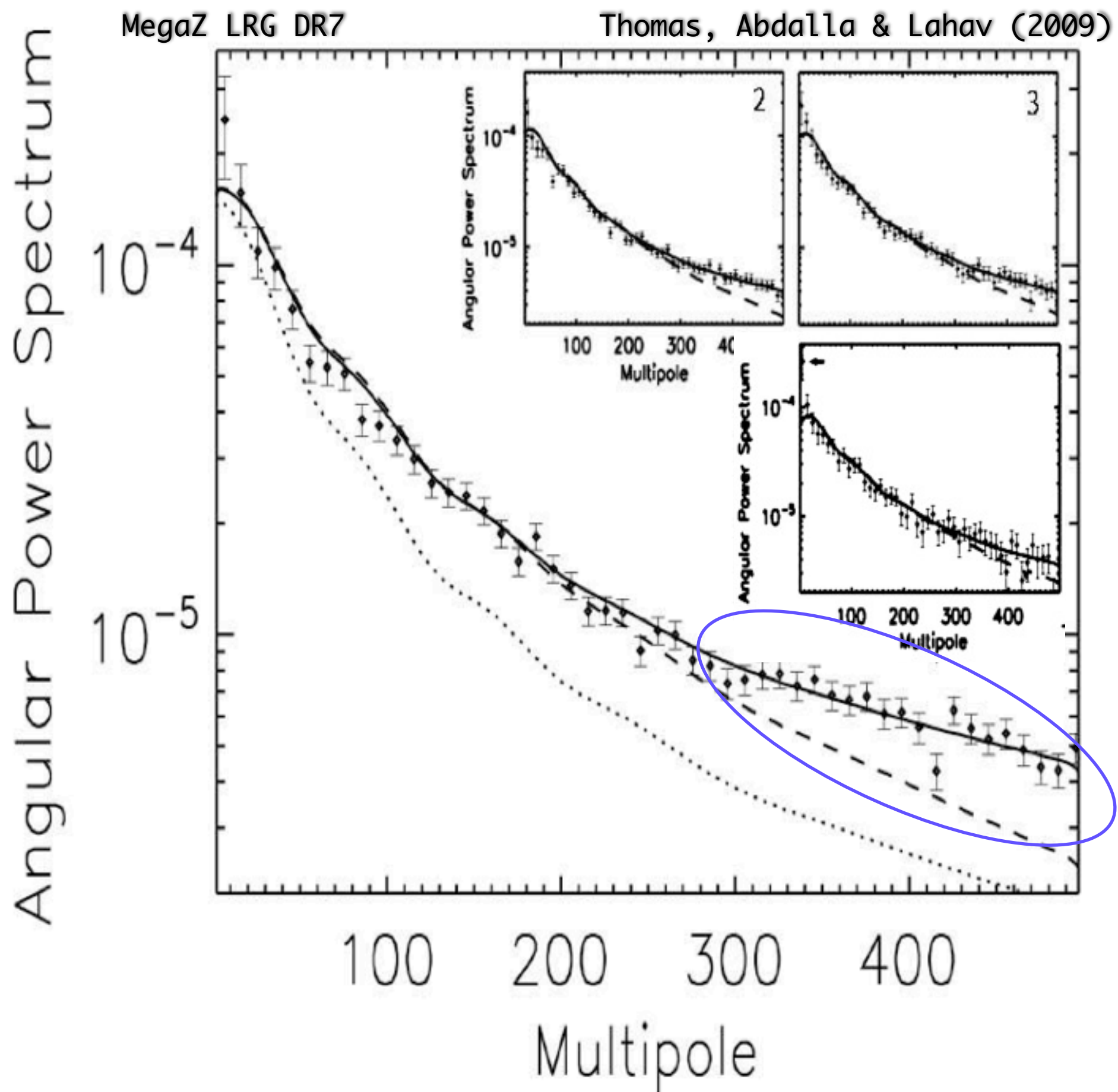


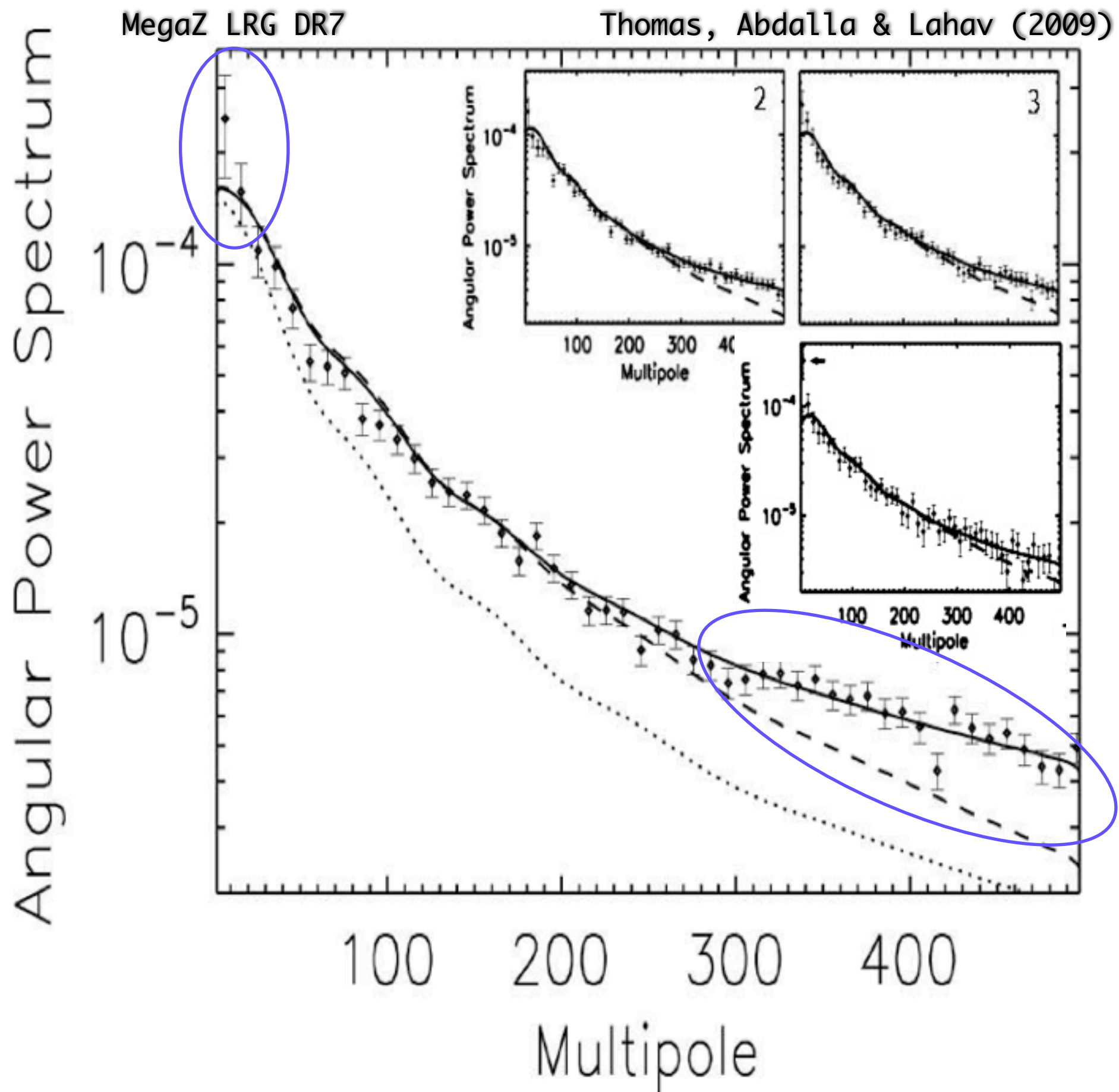


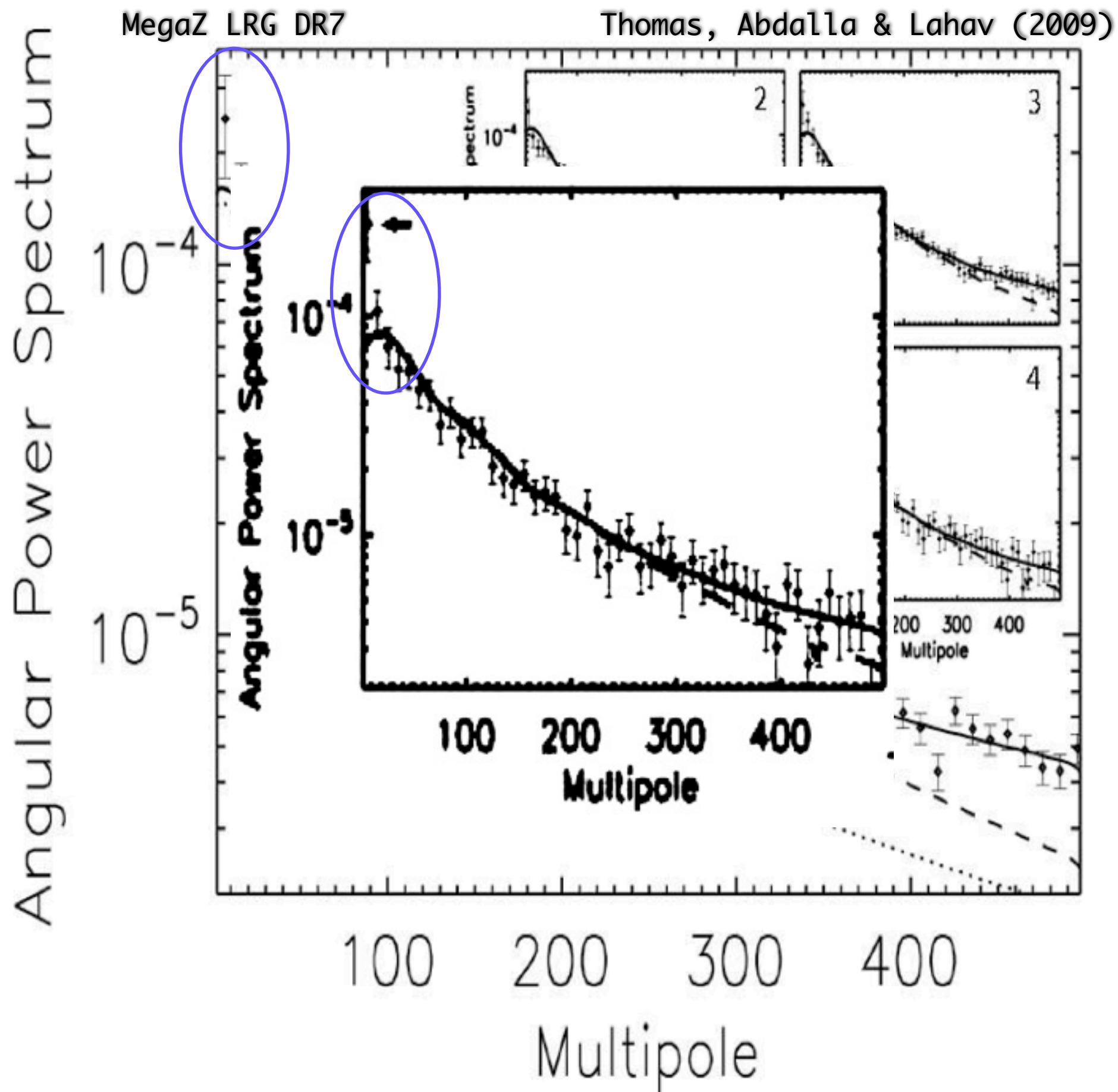
Large Scale Structure in the Local Universe

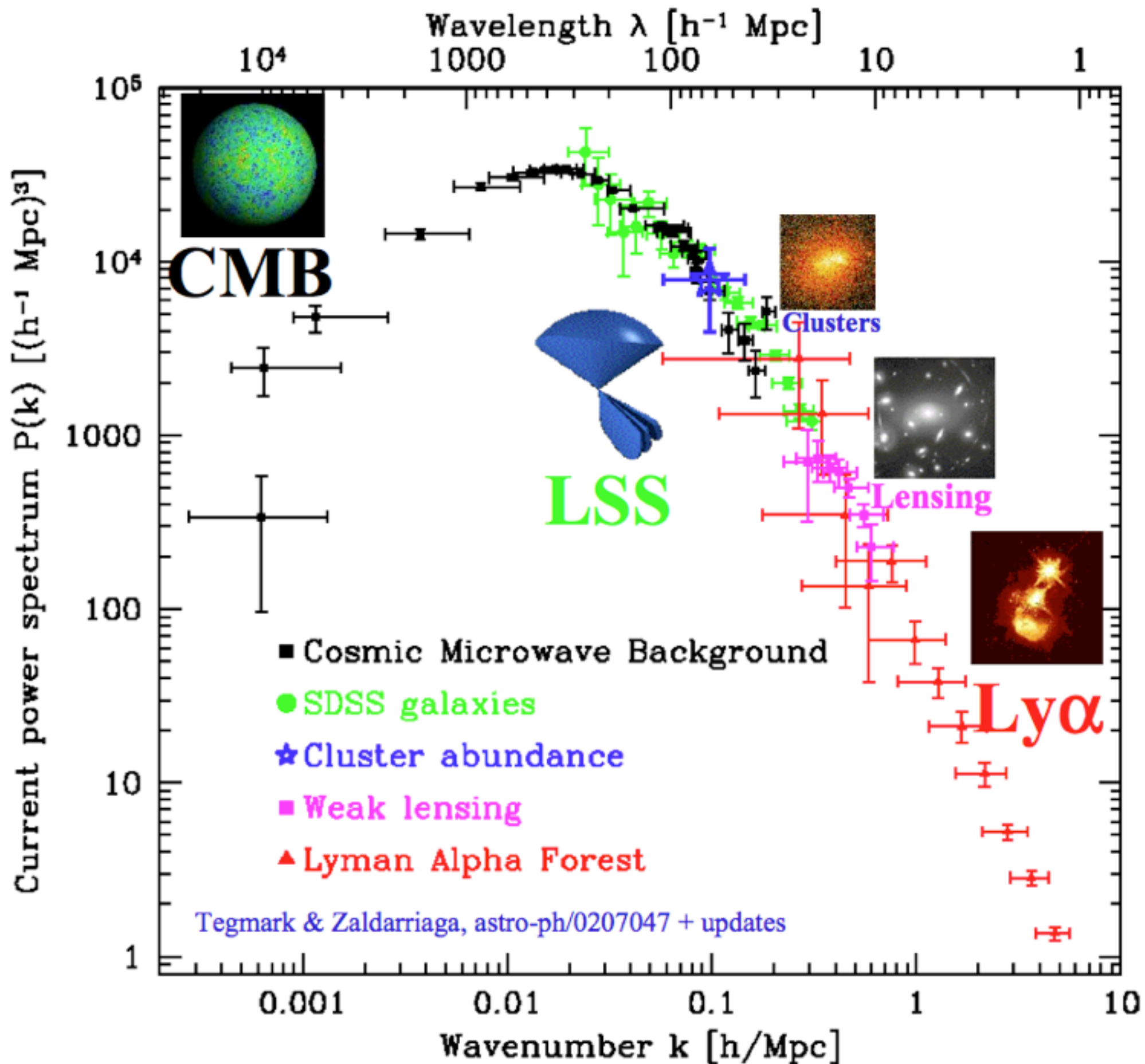


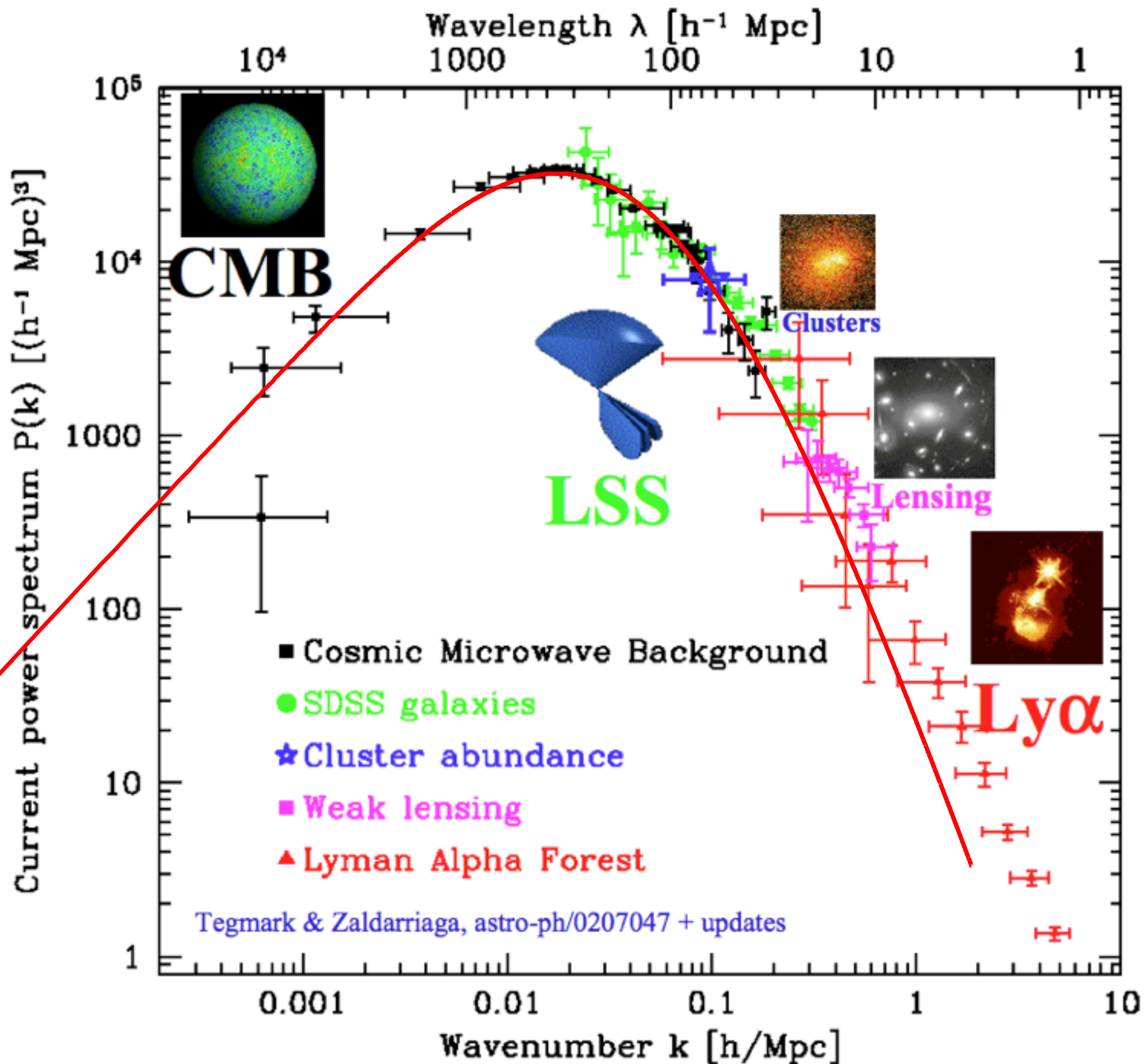


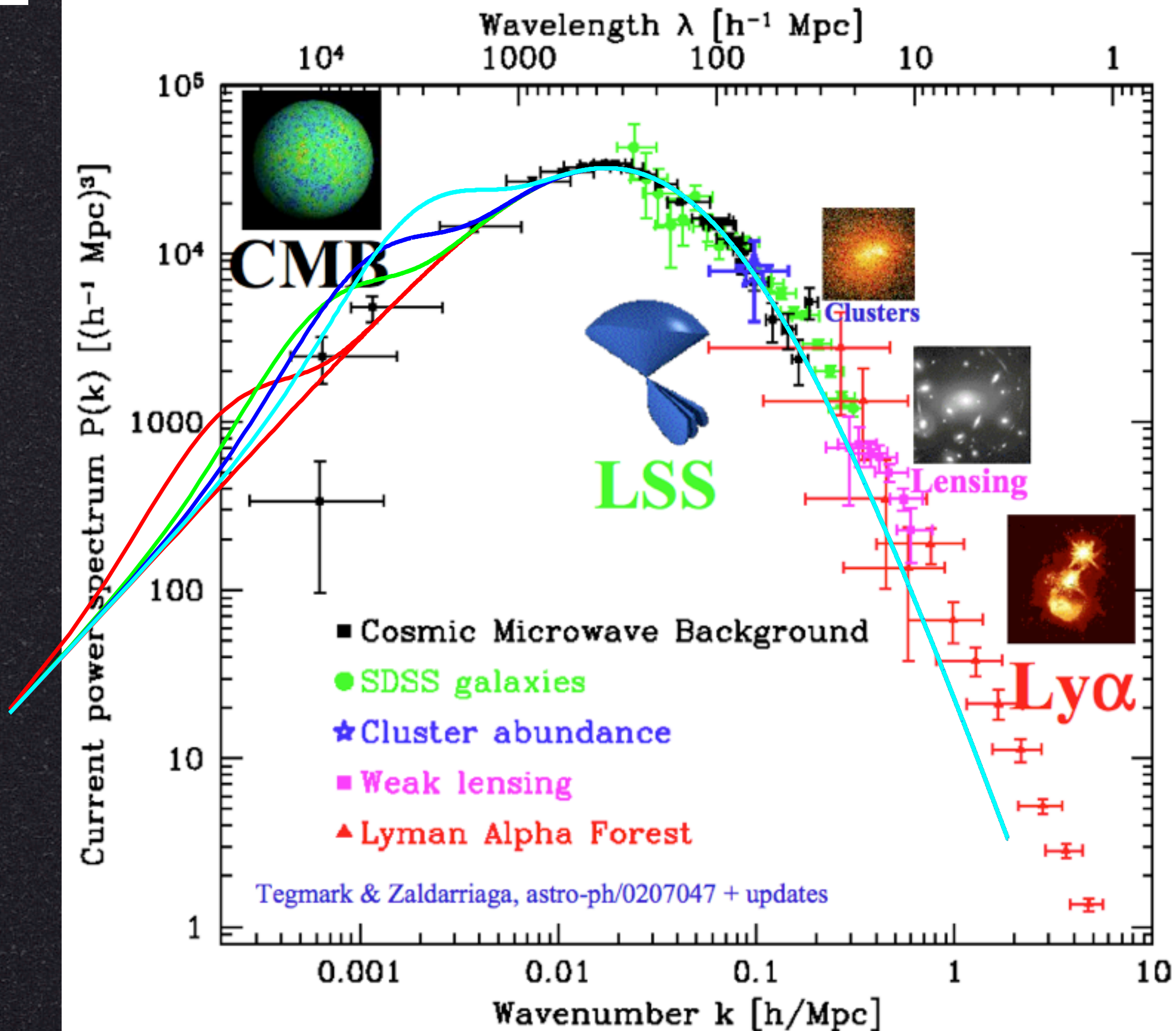


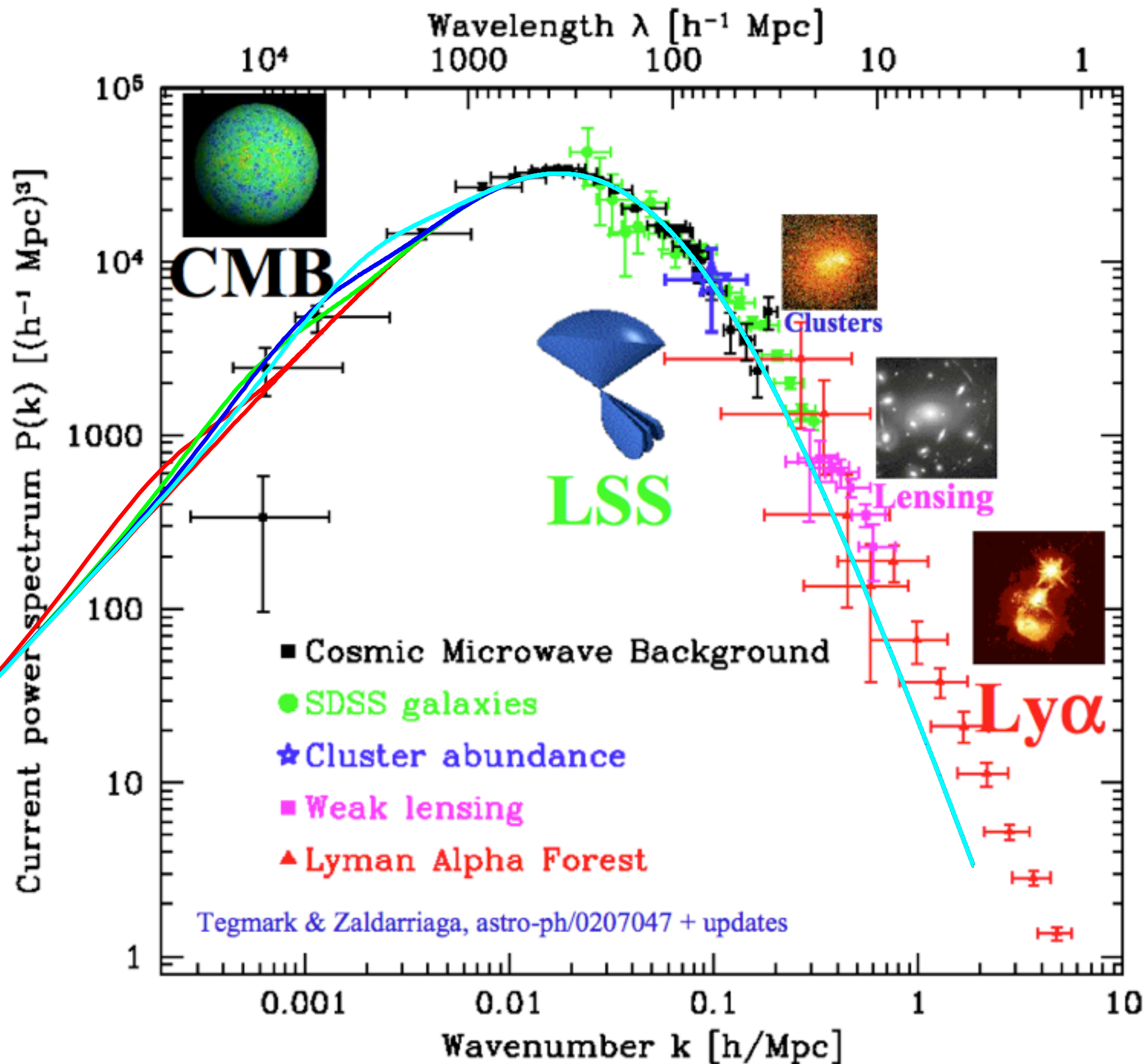












Conclusions

- ✓ Given appropriate window functions, velocity field surveys are consistent with each other.
- ✓ Maximum Likelihood parameter estimation are robust and mostly agree with other methods.
- ✓ There is a minimal sensitivity to small-scale aliasing which biases the results, hiding large-scale flows
- ✓ Optimization of window functions removes the bias and shows the flow
- ✓ Bulk flow disagrees with the Standard Λ CDM parameters (WMAP5) to $\sim 3\sigma$
- ✓ More power on $k \lesssim 0.01$ will make these results likely

Thank you